CHARACTERIZATION OF ENTERIC NERVOUS SYSTEM RESPONSE TO DISEASE CONDITIONS IN INTESTINE

A THESIS SUBMITTED TO
THE GRADUATE SCHOOL OF ENGINEERING AND SCIENCE
OF BILKENT UNIVERSITY
IN PARTIAL FULFILLMENT OF THE REQUIREMENTS FOR
THE DEGREE OF
MASTER OF SCIENCE
IN
MOLECULAR BIOLOGY AND GENETICS

By

Nagihan Gizay Gönüllü

January 2022

CHARACTERIZATION OF ENTERIC NERVOUS SYSTEM RESPONSE TO DISEASE CONDITIONS IN INTESTINE

By Nagihan Gizay Gönüllü

January 2022

We certify that we have read this thesis and that in our opinion it is fully adequate, in scope and in quality, as a thesis for the degree of Master of Science.

Bahar Değirmenci Uzun (Advisor)

Onur Çizmecioğlu

Petek Korkusuz

Approved for the Graduate School of Engineering and Science:

Ezhan Karaşan

Director of the Graduate School

ABSTRACT

Characterization of Enteric Nervous System Response to Disease Conditions in Intestine

Nagihan Gizay Gönüllü

M.Sc. in Molecular Biology and Genetics

Advisor: Bahar Değirmenci Uzun

January 2022

Small intestine is one of the vital organs in gastrointestinal tract that is responsible for absorption of food, amino acids and create barrier against microbial invasion. Whereas large bowel is involved in the reabsorption of water and minerals. Intestinal epithelium is a highly regenerative tissue that it can renew its cells in a span of 4-5 days. In homeostatic state, the turnover rate of the epithelial cells is stable however, in case of inflammation and disease, the rate of proliferation and differentiation increase to regenerate the damaged tissue. Primary cilia (PC) are non-motile, microtubule-based organelles that extrude from plasma membrane. It functions as a sensory element to detect environmental cues. One of the highly studied disease models is ulcerative colitis is mainly characterized by the inflammation of the intestinal mucosal layer and generated by DSS administration. Additionally, high fat diet induced obesity, as a metabolic disease model, was shown to affect intestinal stem cell activity such that higher fat composition of diet causes shortening of small intestine and decrease in weight of tissue. Enteric nervous system is the endogenous nervous network surrounding the gastrointestinal tract and it controls many vital functions including digestion, blood flow, intestinal motility. The initial aim of this study was to reveal the response of intestinal stem cell niche in those stated disease conditions. After detecting ACOT7 protein as a global marker for enteric nervous system of myenteric and submucosal plexus layers, we hypothesized that subpopulations of ENS cells have a connection with intestinal niche upon disease states. Our following goal was to identify subpopulations of ENS and ciliated cells. In order to assess our hypotheses, we conducted series of IHC experiments and confocal microscopy analyses. We found that ACOT7+ cells in ENS contain mainly distinct types of neuronal cell populations such as PHOX2B+ and HuCD+ cells. Further, we identified that glial cells are the main subpopulation of ENS changing their expression pattern in both colitis and obesity models. Also, we classified ciliated cells as a heterogenous population to be colocalized with several ENS and mesenchymal markers. Lastly, we analyzed the gut-brain axis response to DSS induced colitis

in the brain of model animals with a focus on thalamus and insular cortex. We identified several thalamic regions showed similar expression pattern alterations which were observed in colon. Overall, the novelty of this thesis arises from the identification of ACOT7 as an ENS marker along with the detection of glial cell interaction with mesenchymal sub-populations. This interplay demonstrates a response upon disease states of both small intestine and colon.

Keywords: Intestine, enteric nervous system, ACOT7, stem cell, neuron and glial cells, primary cilia, obesity, colitis

ÖZET

Enterik Sinir Sisteminin Bağırsakta Hastalık Durumlarına Cevabının Karakterizasyonu

Nagihan Gizay Gönüllü

Moleküler Biyoloji ve Genetik, Yüksek Lisans

Tez Danışmanı: Bahar Değirmenci Uzun

Ocak 2022

İnce bağırsak, gıdaların, amino asitlerin emiliminden sorumlu olan ve mikrobiyal istilaya karşı bariyer oluşturan sindirim sistemindeki hayati organlardan biridir. Bunun yanı sıra kalın bağırsak başlıca su ve mineral emiliminde rol oynar. Bağırsak epiteli yüksek oranda yenilenebilen bir doku olup, tüm hücrelerini 4-5 günlük bir süreçte yenileyebilir. Özdenge durumunda, epitel dokudaki hücrelerin yenilenme ve ölme oranları sabitken; bağırsakta iltihap oluşumu ve hastalık durumlarında, hücre bölünme ve yenilenme hızı zarar görmüş dokuyu onarmak amacıyla artmaktadır. Primer silya mikrotübül temelli bir organel olup hücre zarından dışarı doğru uzantılar oluşturmaktadır. Çevresel sinyallerin algılanmasında görev alır. En çok çalışılan hastalıklardan biri olan Ülseratif Kolit, kalın bağırsağın epitel dokusunun enflamasyonu ile tanımlanır ve DSS kimyasalı ile fare modelinde oluşturulur. Bununla beraber, yüksek yağlı beslenmeyle oluşturulan obezite bir metabolik hastalık modeli olarak kullanılmakla beraber bağırsak kök hücrelerinin aktivitesinin yüksek yağ oranından etkilendiği gösterilmiştir. Bu etki bağırsak boyunda kısalma ve dokunun ağırlığının azalması şeklinde gözlemlenmiştir. Enterik sinir sistemi sindirim sistemini saran endojen bir sinir sistem ağı olup, sindirim, kan akışı ve bağırsak hareketliliği gibi birçok hayati fonksiyonu kontrol eder. Bu araştırmanın birincil amacı kök hücre nişinin belirtilen hastalık durumlarındaki reaksiyonunu ortaya koymaktır. ACOT7 proteinini miyenterik pleksus ve submukozal pleksuslardan oluşan enterik sinir sisteminin evrensel bir belirteci olarak saptadıktan sonra hipotezimiz enterik sinir sistemi hücrelerinin alt popülasyonlarının hastalık durumunda bağırsak nişi ile bağlantısı olduğu yönünde şekillendirildi. Bunu takip eden amacımız enterik sinir sistemi alt hücrelerini ve primer silya yapılarına sahip hücreleri tanımlamaktır. Hipotezimizi incelemek için immünohistokimya deneyleri ve konfokal mikroskop analizleri gerçekleştirilmiştir. Böylelikle, enterik sinir sistemindeki ACOT7 pozitif hücreler başlıca belirgin sinir hücre popülasyonlarını içermekte ve bu hücreler HuCD ve PHOX2B proteinlerini pozitif olarak göstermektedir. Ek olarak, obezite ve kolit hastalık modellerinde enterik sinir sisteminin alt gurubu glia hücreleri

ekspresyon davranışları değişen ana hücre gurubu olarak belirlenmiştir. Ayrıca heterojen bir popülasyon olarak primer silya içeren hücrelerin enterik sinir sistemindeki ve mezenkimal dokudaki hücrelerle beraber bulunduğu gözlemlenmiştir. Son olarak, bağırsak-beyin ekseninin DSS ile indüklenmiş kolit modeline cevap vereceği tepkiyi bu modeldeki hayvanların beyinlerindeki özellikle talamus ve insular korteks bölgelerinde inceledik. Bazı talamus bölgelerinin kalın bağırsakta gözlemlenen ekspresyon değişimlerine benzer davranışlar gösterdiğini tespit ettik. Sonuç olarak, bu çalışmanın özgünlüğü ACOT7 proteininin enterik sinir sistemi belirteci olarak tespit edilmesinden ve glia hücrelerinin mezenkimal hücre alt popülasyonlarıyla etkileşiminin ince bağırsak ve kolon hastalık modellerinde gösterilmesinden kaynaklanmaktadır.

Anahtar Sözcükler: Bağırsak, enterik sinir sistemi, ACOT7, kök hücre, sinir ve glia hücreleri, primer silya, obezite, kolit

ACKNOWLEDGEMENTS

I would like to thank my supervisor Asst. Prof. Bahar Değirmenci for her support and guidance throughout this project. Her wisdom and ambition contributed highly to both my academic career and my character as a young researcher. Without her efforts, this thesis would never be accomplished. I will be forever thankful for every single input she provided me in a span of two and a half years. I would also like to thank my brilliant and supportive very best friend and colleague Müge Bozlar for being in every part of my life both academically and personally since our bachelor days. I would like to thank the newest member of our group İlke Sarı for her endless efforts to help me with experiments and data acquisition. Last couple of months became easier thanks to her immense support. I would like to thank our former group member Deniz Esen for her contribution with single cell RNA-sequencing reanalysis.

I would like to thank jury members in my Master's Thesis Committee Asst. Prof. Onur Çizmecioğlu and Prof. Dr. Petek Korkusuz for their contributions.

I would like to thank our veterinary scientists Gamze Aykut and Ulaş Saçıntı for their support in animal experiments. They never ceased to help me whenever I required them to assist me. Also, I would like to thank Prof. Dr. Petek Korkusuz and her group for their continuous support during this thesis. Their collaboration contributed to this thesis immensely.

I would like to thank all my closest friends for their emotional support. Last but not least, I would like to thank my supportive and selfless boyfriend and colleague Orkun Ok for being there for me all the time. Without his tremendous help both in my daily life and in my academic life, I wouldn't come this far and achieve such accomplishments. This thesis is dedicated to my parents Yeşer Gönüllü and Köksal Gönüllü whom I am forever grateful to. I would never have become the person I am today without their relentless dedication in every step of my life.

This work was funded by EMBO installation grant and TÜBİTAK 1001 grant 219Z163 awarded to Dr. Bahar Değirmenci Uzun.

Table of Contents

List of Abbreviations

ACOT7	Acyl-CoA Thioesterase 7
AD	Anterodorsal Nucleus
APC	APC Regulator of WNT Signaling Pathway
ARL13B	ADP- Ribosylation Factor Like Protein 13B
ASC	Adipose Derived Mesenchymal Stem Cell
aSMA	Alpha Smooth Muscle Actin
BMP	Bone Morphogenic Protein
cAMP	Cyclic AMP
CBC	Crypt Base Columnar Cell
CNS	Central Nervous System
DKK3	Dickkopf WNT Signaling Pathway Inhibitor 3
DLL4	Delta Like Canonical Notch Ligand 4
DSS	Dextran Sulfate Sodium
ECM	Extracellular Matrix
EGF	Epidermal Growth Factor
ENS	Enteric Nervous System
ER	Endoplasmic Reticulum
FGF	Fibroblast Growth Factor
FOXL1	Forkhead Box L1
GLI1	GLI Family Zinc Finger 1
GPCR	G-Protein Coupled Receptor
GSK3	Glycogen Synthase Kinase 3
HFD	High Fat Diet
IBD	Inflammatory Bowel Disease
IHC	Immunohistochemistry
IHH	Indian Hedgehog
InsCtX	Insular Cortex
ISC	Intestinal Stem Cell

JAG2	Jagged Canonical Notch Ligand 2
KIF	Kinesin Family Member
LGR5	Leucine-Rich Repeat-Containing G-Protein Coupled Receptor 5
LRP	LDL Receptor Related Protein
mTORC1	Mammalian Target of Rapamycin Complex 1
MUC2	Mucin 2
OLFM4	Olfactomedin 4
PC	Primary Cilia
PCNT	Pericentrin
PDGFRA	Platelet Derived Growth Factor Receptor A
PHOX2B	Paired Like Homeobox 2B
PTCH	Patched
PVT	Periventricular Nucleus of Thalamus
RNF43	Ring Finger Protein 43
RSPO1	R-spondin 1
RTK	Receptor Tyrosine Kinase
S100beta	S100 Calcium Binding Protein B
SHH	Sonic Hedgehog
SMO	Smoothened, Frizzled Class Receptor
SOX9	SRY-Box Trancription Factor 9
SOX10	SRY-Box Trancription Factor 10
TA	Transiently Amplifying Cells
TUJ1	Tubulin Beta 3 Class III
ZNRF3	Zinc and Ring Finger 3

1. INTRODUCTION

1.1 Small Intestine and Colon

Small intestine is one of the vital organs in gastrointestinal tract that is responsible for absorption of food, amino acids and create barrier against microbial invasion whereas large bowel is mainly responsible for reuptake of water and minerals (Kong, Zhang, and Zhang, 2018). Intestinal epithelium is a highly regenerative tissue that it can renew its cells in a span of 4-5 days. In homeostatic state, the turnover rate of the epithelial cells is stable however, in case of inflammation and disease, the rate of proliferation and differentiation increase to regenerate the damaged tissue (Büller et al, 2012). The structure of small intestine is in the shape of enclaves and exclaves, namely the crypts and villi, to increase the surface area to facilitate nutritional uptake. Large intestine lacks villus structures and its crypts are embedded into the mesenchymal layer (Simons and Clevers, 2011; Kong, Zhang, Zhang, 2018). Intestines are formed by a single layer of epithelial cells and sub epithelial mesenchymal cells. Epithelial cells are composed of multipotent intestinal stem cells and differentiated cells such as enterocytes, Goblet cells etc. In small intestine, at bottom of the crypt, stem cells are located with a dispersed population of Paneth cells which move downwards during differentiation while other types of cells migrate out of stem cell zone to generate villi structure. In the colonic crypts, because Paneth cells are absent, there is no main epithelial niche. Rather they contain larger number of secretory cells like Goblet cells (Barker 2014). Enterocytes comprise the majority of the cells in the epithelial layer. They are responsible for nutrient absorption as well as secretion of immunoglobulins as a part of immune mechanism. Goblet cells mainly produce mucus layer to cover exterior surface of the small intestine so that epithelial cells are not disrupted by absorptive enzymes (Kong, Zhang, and Zhang, 2018). Such differentiated cells excrete factors to negatively regulate the size of the compartments and stem cell zonation. In a damage condition, these signals decrease to accelerate proliferation rate (Büller et al,2012).

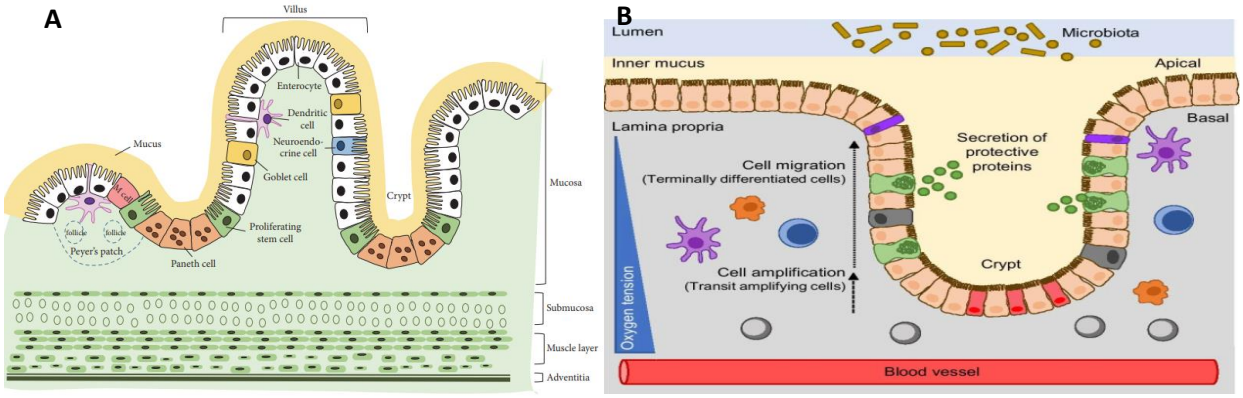

Figure 1: Small intestinal (A) and colonic structures (B) (Kong, Zhang, and Zhang, 2018; Ternet and Kiel,2021).

1.2 Intestinal Stem Cells

The regenerative capacity of intestine arises from profound activity of multipotent stem cells. There are two types of stem cells in small intestine: crypt base columnar cells and quiescent +4 cells. The latter are located on the +4 position from crypt base and establish a reserve stem cell population while the former is the main stem cell reservoir to generate all types of intestinal cells (Clevers and Bevins, 2013). They initially proliferate to yield transiently amplified cells which are progenitors to further differentiate into all lineages. Initially, the actively cycling cells in small intestine is defined as crypt base columnar (CBC) cells because they are able to maintain epithelium in long term by self-renewing. Barker et al. first described a very specific marker, namely Lgr5, in small intestine and colon to identify adult CBC cells by single cell RNA sequencing. This marker is a receptor for Wnt agonist R-spondin, enhancing the signaling. It is also a Wnt target gene which enable positive regulation of stemness (Barker et al,2007). Because it is unique to CBC cells, Lgr5 can be used to differentiate stem cells from transiently amplifying cells and Paneth cells. Lgr5+ CBC cells can be located in stem cell permissive environment which is controlled by various factors, and they are adjacent to Paneth cells (Clevers and Bevins, 2013). Because Lgr5 is a transcription factor and located in the nucleus of the cells, it is hard to detect in cellular level. Thus, an alternative stem cell marker was identified in small intestine and colon, namely Olfm4. This marker is highly robust and specific for CBC cells (Van der Flier et al, 2009). As opposed to small intestine, colon has no villi structure however stem cells exist at the bottom of the crypts (Clevers and Bevins, 2013). Stem cells can also be identified with Lgr5 marker gene at the colonic crypts (Barker et al, 2007). Even though both colonic and intestinal stem cells are marked by Lgr5 expression, colonic CBCs are found to be more quiescent than small intestinal stem cells (Barker et al,2007).

1.3 Stem Cell Niche

Previously mentioned, intestinal epithelium has a high regenerative capacity such that it can replenish itself in every three days with the help of actively proliferating stem and progenitor cells at the bottom of crypts. The defined structure of small intestine and colon during homeostasis is balanced by loss of differentiated cells from the top of the villi in parallel with proliferation (Barker et al,2007). In general terms, stem cell niche creates a microenvironment by complex interaction of supporting cells and extracellular matrix (Scadden 2006). Higher regeneration rate of intestinal stem cells is provided by core ligands secreted by niche components (Degirmenci et al,2018; Barker et al,2007).

1.3.1 Basic Stem Cell Niche: Paneth Cells

The capacity of stem cells to actively proliferate in small intestine is provided by Paneth cells which comprise one of the differentiated cell lineages. These cells are mainly responsible for forming stem cell niche by producing main driver factors. Paneth cells are situated at the bottom of the crypt, between Lgr5+ stem cells. Their turnover rate is less than other types of cells therefore Paneth cells can reside around 1 months at their location. The main driver for proliferation along the intestinal crypts is Wnt. Fundamental niche factors for Lgr5+ stem cells are EGF, Wnt3, Notch ligand and Dll4, all are mainly presented by Paneth cells. Along with the production of niche factors, Paneth cells are responsible for secretion of antimicrobial peptides specifically α- defensins and involved in protein synthesis (Kong, Zhang, and Zhang, 2018). The importance of Paneth cells on stemness has been shown with several depletion assays such that Paneth cell loss causes Lgr5+ stem cell destruction leading to a decrease in regenerative capacity (Sato et al, 2011). Additional to providing stem cell niche, Paneth cells have a role as nutrition sensor in small intestine. Depending on nutrition absorption, stem cell activity can be increased by mTORC1 inhibition in Paneth cells. Usage of TOR inhibitor rapamycin can be used to enhance niche activity of Paneth cells by mimicking calorie restriction (Yilmaz et al,2012; Clevers and Bevins, 2013).

1.3.2 Extraepithelial Niche

Small intestine is formed by single epithelial layer including Lgr5+ stem cells, Paneth cells which is considered as main niche element and various differentiated cells. However, studies that ablate Wnt3 factor specifically in epithelial layer showed no change in the stem cell activity. This result brings about a notion that secondary Wnt signals are provided by non-epithelial sources (Farin and Clevers, 2012). Further investigations indicated that subepithelial

layer, namely mesenchyme, has undeniable importance to sustain intestinal stem cell activity. Mesenchymal cells are situated under epithelium surrounding both crypts and villi. During development and homeostasis, activators and inhibitors of stem cell driver factors including Wnt, Hedgehog should be coordinated to generate architecture of the small intestine accurately. Thus, several Wnt inhibitory factors are secreted from both Paneth cells and extraepithelial cells along with the Wnt agonists to preserve crypt villus zonation. This polarity is maintained by the gradient of Wnt/BMP provided by both epithelial and mesenchymal cells. Although mesenchymal cells can be categorized as smooth muscle cells, pericytes and myofibroblast, more heterogenous cell populations generate this layer (McCarthy et al, 2020). Main colonic niche is formed by extraepithelial cells secreting Wnt, Notch and EGF (Barker et al,2007).

As the researchers divert their attention to point out these populations, distinct markers and essential roles of these cells begin to be revealed. PDGFRA is one of the markers defining a mesenchymal cell population which generates a gradient along the crypt villus axis, and it is shown to be required for villus formation. McCarthy et al. defined two distinct intestinal cell types which can be marked by PDGFRA, namely $CD81^-$ stromal cells and Trophocytes. Additionally, $PDGFRA^{high}$ telocytes are located at the base of the villi and provide BMP signal. BMP is a Wnt antagonist that blocks the proliferation and induces differentiation so that it controls the crypt size and generates villus structure. Another cell type marked by PDGFRA is $CD81^+$ $PDGFRA^{lo}$ trophocytes located below the crypts. These cells were found to secrete Gremlin 1, a BMP inhibitor, and Wnt2b favoring the stem cell activity. Strikingly, trophocytes were detected to be sufficient to promote proliferation of stem cells in *in vitro* conditions with an addition of several trophic factor showing that these subpopulations of cells can provide the niche for intestinal stem cells. Also, it is demonstrated that BMP inhibition leads to ectopic stem cell activity resulted in crypt formation along the villus direction. When expression of BMP inhibitor was increased, Gremlin1 activity was also enhanced causing an acceleration in proliferation rate and increased risk for colorectal cancer. Therefore, this homeostasis between mitotic activity and differentiation is maintained by these specific clusters of PDGFRA expressing cells creating a BMP/Wnt gradient such that pericryptical zone is enriched in Wnt and R-spondin while cells in villus lamina propria secrete more BMP signals than Wnt/R-spondin (McCarthy et al, 2020).

Aside from PDGFRA subset of cells, Foxl1 is another identified marker for mesenchymal fibroblast population. These Foxl1+ cells are involved in the niche for ISCs although they diverge from myofibroblasts and smooth muscle cells. They are mainly located in close

proximity to epithelial membrane of the crypt base and they highly express Wnt2b, Wnt5a, R-spondin3, FGF, Gremlin1/2 and BMP antagonist. Interestingly, depletion of Foxl1+ cells lead to drastic reduction in proliferative capacity of both ISCs and TA cells along with disruption of epithelium even though Paneth cell ablation doesn't show any change in the stem cell function. Further, Foxl1+ cell loss was shown to change the structure of small intestine and colon resulted from decreased villus length and reduction in depth of colonic crypts. The factors expressed in Foxl1+ cells and canonical Wnt signaling are also decreased upon depletion of these cells (Aoki et al, 2016). A different study on Foxl1+ mesenchymal cells suggests that they can express Wnt inhibitors including DKK3, BMP4, BMP5 as well as BMP inhibitor Gremlin1. This dispersed population of Foxl1+ cells confirms the crypt villus axis by regulating the expression of activator and inhibitor signals of proliferation depending on the localization of cells in that axis (Shoshkes-Carmel et al, 2018).

Because Wnt ligand is the major driver of the intestinal stem cell activity, global loss of Wnt have shown to result in depletion of crypt and aberrant formation of villus structure accompanied by decrease of stemness markers including Lgr5, Olfm4, Troy. Although Paneth cells are the basic source for Wnt signal for small intestine, epithelial specific depletion of Wnt ligand in mice showed that small intestinal stem cells of these animals were able to maintain self-renewal due to Wnt ligands supplied by mesenchymal cells (Valenta et al, 2016). Degirmenci et al. identified a subpopulation of mesenchymal cells that can be marked by Gli1 transcription factor expression. They are also located in close proximity to crypt base and provide an extraepithelial Wnt source for ISCs. Upon DSS treatment, number of Gli1+ cells were shown to be increased in order to provide recovery and restoration of proliferative capacity in colon. Similar to colon, number of Gli1+ cells were shown to be enhanced upon epithelial depletion of Wnt ligand in small intestine. Thus, Gli1+ cells which is a subset of mesenchymal cells provide a reserve niche for both small intestinal and colonic stem cells (Degirmenci et al, 2018). Considering these distinct but heterogenous cell populations, intestinal stem cell niche is composed of a complex and multi-factorial communication between diverse cell types and secreted environmental cues thus, further comprehensive analysis is required to reveal complete interaction and function.

1.3.3 Niche Factors: Main Drivers Wnt and Hedgehog Signaling Pathways

Stem cell activity strictly depends on initiation of signaling cascades by ligands secreted from Paneth cells and mesenchymal cells in the stem cell niche. The major driver for stemness is canonical Wnt/beta catenin signaling. It is a growth factor which enables cell proliferation. It is

involved in the regulation of gene expression profile which shapes the growing tissue by cytoskeleton function (Sawa 2012; Nusse and Clevers, 2017). It is a signal molecule acting in a paracrine fashion. Different subtypes of Wnt ligand are used in various tissues in the body. For example, Wnt1 knock out leads to midbrain abnormalities while Wnt4 depletion causes problems in kidney development (McMahon et al,1992; Stark et al,1994). During production, Wnt is modified via palmitoylation on ER by porcupine which is a palmitoyl transferase. This lipid tethering to Wnt functions as a binding motif to attach to the target cell membrane. However, by making Wnt hydrophobic, it limits the distance for Wnt ligands to diffuse so that signal can be transferred to close proximity from the Wnt producing cell. Wnt requires a transmembrane protein to carry its mature form to plasma membrane for secretion, namely Wntless/Evi. Although, it remains unclear that how hydrophobic Wnt molecule is transported to target cells, one speculation could be the existence of a sequential signaling path among Wnt molecules. After secretion, Wnt binds to its receptor Frizzled generating a complex with LRP5/6. Dimerization of receptors upon ligand binding leads to phosphorylation of cytoplasmic tail of LRP5/6 by GSK3 which in turn recruits Axin, the scaffold protein. Upon this interaction, destruction complex comprised of Axin, beta catenin, APC and 2 serine/ threonine kinases becomes disrupted. Due to this disengagement, beta catenin stays stabilized and free to migrate into nucleus. By binding of beta catenin to transcription factor TCF in nucleus, the expression of target genes is enhanced. When Wnt cascade is in off state, beta catenin is degraded by proteasome in destruction complex while TCF remains bound to Groucho which switches TCF into a transcriptional repressor. Even though activation of Wnt signaling pathway is fundamental to provide stem cells with proliferative capacity, it is not sufficient to fully potentiate the self-renewal of Lgr5+ stem cells such that R-spondin is required. R spondins are Wnt agonists that can associate with Lgr5 family member receptor in order to augment signaling. They are known to remove membrane factors, namely Znrf3 and Rnf43, involved in lysosomal destruction of Wnt so that R spondins increase stability of Wnt receptor binding. Specifically, RSPO1 was found to support intestinal crypt proliferation by Wnt ligand (Nusse and Clevers, 2017). Because Wnt ligand is the major element for stemness, any inhibitory effect causes abnormalities in the homeostatic state and regenerative activity in small intestine and colon. One of the Wnt antagonists that were shown to affect stem cell activity are the Dkk family members. Dkk1 interacts with Wnt coreceptor and blocks the expression of target genes leading to cessation of proliferative activity in both small intestine and colon. As a result, structure of the tissue was disrupted while crypt and villus were found to be depleted (Kuhnert et al, 2004, Aoki et al, 2016). Another notable inhibitor for Wnt is Notum which acts to remove

palmitoleate modification from the ligand. It has been shown that increased Notum production by Paneth cells in the aged epithelium could be the cause of the decline in regenerative capacity It was also suggested that targeting Notum or extracellular addition of Wnt can restore the stemness of aged epithelial cells (Pentinmikko et al, 2019).

Even though Wnt is vital to maintain stem cell function, Hedgehog pathway also plays a very crucial role to balance regeneration and differentiation. The main Hedgehog ligand in small intestine and colon is Indian Hedgehog (Ihh). As opposed to Wnt ligand, it is produced from differentiated epithelial cells to act upon mesenchymal cells generating a negative feedback mechanism. Thus, smooth muscle cells, pericytes and myofibroblasts are among Hh responsive cells in small intestine (Büller et al, 2012). Patched (Ptch) is the main receptor for hedgehog ligands and in the absence of Hedgehog ligand, Ptch blocks the activation of signaling receptor SMO. As a result, GLI family members undergo partial cytoplasmic degradation, leaving an intact N terminus to repress transcription. Upon initiation by ligand, SMO inhibition by Ptch is attenuated so that SMO can lead to GLI translocation to nucleus and activation of its target genes such as GLI1, PTCH1, FOXL1 and JAG2 (Katoh and Katoh, 2006). Hedgehog signaling is responsible for negatively regulating proliferation rate of stem cells and crypt size as well as preserving and augmenting mesenchymal cell population to provide homeostasis. Proposed model for negative regulatory loop by Büller et al. describes that Ihh ligand secreted from differentiated epithelial cells can trigger mesenchymal cells to produce BMP and Activin which limits the proliferation of stem cells and promote differentiation. These factors secreted from upper regions of crypt villus axis can act to suppress Wnt ligand produced at the bottom of the crypt. Ihh depletion has been shown to induce aberrant proliferation of stem cells resulting in generation of crypt like structures at abnormal locations. Further, inflammation and villus degeneration were observed upon Ihh loss (Büller et al, 2012). Therefore, signals produced from different regions of the small intestine, mainly Wnt and Ihh, work in coordination to preserve the structure and innate functions of the specific cell types.

1.4 Enteric Nervous System

Gastrointestinal tract involving small intestine and colon have endogenous nervous system called enteric nervous system (ENS). It is a component of peripheral nervous system, but it functions similar to central nervous system (Gabella 1981; Gershon 1997; Iruzubieta et al,2020). ENS has several vital roles in the normal functioning of intestines. It mediates digestion via regulating bowel movements, coordinates and interacts with immune cells and holds a barrier against microbial community (Yoo and Mazmanian, 2017; Drokhlyansky et

al,2020). ENS is formed by complex interactions of enteric glial cells and neurons spanning the muscular layer of intestinal tissue (Junquera et al. 2011; Furness 2012; Iruzubieta et al,2020). These complexes are mainly found in two layers; myenteric plexus and submucosal plexus (Furness 2012; Iruzubieta et al,2020). Any damage in the integrity of enteric nervous system leads to several metabolic diseases and neuropathies including Hirschsprung's disease, Parkinson's disease and gut motility disfunctions (Furness 2012; Drokhlyansky et al,2020). Enteric glial cells form the main cell populations of ENS, and they can be found in the extra-ganglionic sites including mesenchymal layer (Baghdadi et al,2021; Gulbransen and Sharkey, 2012; Rühl 2005). Neuron and glial networks extend from myenteric and submucosal plexus toward the mucosal lamina propria. Majority of glial cells in the myenteric plexus are marked by S100beta, Sox10 (Rao et al,2015; Baghdadi et al,2021). Neurons in the plexuses of the intestines can be marked by common neuron marker HuCD, neuron fiber marker Tuj1 (Morarach et al, 2021; Graham et al, 2020). Single cell level analysis of enteric nervous system demonstrates the complexity and heterogeneity of neuronal and glial cell functions and interactions.

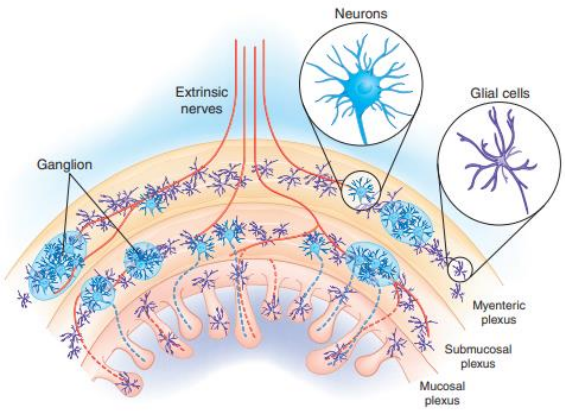

Figure 2: The structure of enteric nervous system. It constitutes a complex interaction of neurons and glial cells forming bundles called ganglions in myenteric plexus (the outer layer) and submucosal plexus located underneath the mesenchymal and epithelial layers. These neuronal and glial cells extend towards the lamina propria forming mucosal plexus (Rescigno 2008).

1.4.1 ACOT7 Enzyme in Nervous System

ACOT (acyl-CoA thioesterase) enzyme clusters are involved in the hydrolysis of acyl-CoA to free fatty acids. They also coordinate the concentration and localization of free fatty acids in several tissues (Ellis et al,2015). These enzymes are involved in the lipid metabolism and their lack or disruption cause several metabolic diseases such as fatty liver, insulin resistance and obesity shown by some knock out studies (Ohtomo et al,2013; Kang et al,2012; Zhang et al,2012; Zhuravleva et al 2012). Specifically, ACOT7 is known to be cytosolic and have a predominantly higher enzymatic activity than other ACOT cluster enzymes in cellular fatty acid metabolism (Yamada et al, 1994; Kuramochi et al,2002; Yamada 2005; Ohtomo et al,2013). Further, ACOT7 is highly expressed in the neurons thus it constitutes the main enzyme for

hydrolysis of long chain fatty acids in the brain. Elimination of ACOT7 specifically in the brain demonstrates physiological and metabolic phenotype similar to neurodegeneration. These changes were shown to be deteriorated upon fasting in which free fatty acid levels are increased (Ellis et al,2013). These prior data suggest ACOT7 to be functional in metabolic changes related to fatty acid alterations in several tissues.

1.4.2 Gut-Brain Axis: Enteric Nervous System to Brain Connection

Brain as a component of central nervous system collects information by both neuronal and endocrine stimuli from peripheral organs in the gastrointestinal tract. The gut-brain axis stands for the bidirectional signal relay between central nervous system and enteric nervous system via hormonal secretions or neural transmission (Romijn et al,2008; Rhee et al,2009; Agusti et al,2018). This communication pathway functions mainly in regulating digestive behaviors such as hunger-satiety, food absorption, glucose and insulin balance and fat metabolism (Cryan et al,2019; Romijn et al, 2008). Even though enteric nervous system can act autonomously independent from brain, parasympathetic and sympathetic nerves contribute to the interplay between brain and gut to exert these vital functions (Romijn et al, 2008). Recent studies suggest that dysregulation of this tight interaction between gut and brain could be the root for the cognitive and psychological outcomes of inflammatory and metabolic diseases in the gastrointestinal tract (Cenit et al., 2017; Singh et al., 2017; Agusti et al,2018). For instance, obese individuals commonly display psychological effects such as depression or anxiety in addition to some cognitive deficits in learning abilities and memory (Yang et al,2016; Agusti et al, 2018). Further, a recent study suggests that neurons in the specific region of the brain are activated upon inflammation in the colon induced by dextran sulfate sodium administration. These neurons generate a hub collecting immunological cues from the peripheral organs specifically colon in this case. This shows the importance and directness of the interaction between gut and the distinct brain regions (Koren et al,2021). Mechanisms and interaction pathways are still under close investigation.

1.5 Primary Cilia

Primary cilia (PC) are non-motile, microtubule-based organelles that extrude from plasma membrane. They function as a sensory element to detect environmental cues. Their structure is composed of a basal body from which the structure is generated and anchors primary cilia to the cell membrane, and axonome extending from the basal body. It is also covered by lipid bilayer as an extension of cell membrane (Pedersen et al, 2016). Primary cilia can be found in

majority of all vertebrate cell types including epithelial tissue, connective tissue, muscle cells and neurons. Axonome structure is responsible for migration of signaling molecules and receptors from cytoplasm to cell membrane or vice-versa. Anterograde motion is movement of molecules from base of the primary cilia towards the tip and it is performed by Kinesin 2 complex proteins including KIF3a, KIF3b and KAP3 while retrograde motion defines the transport of molecules from tip to base of the primary cilia carried out by dynein 2 motor proteins (Bangs and Anderson, 2017).

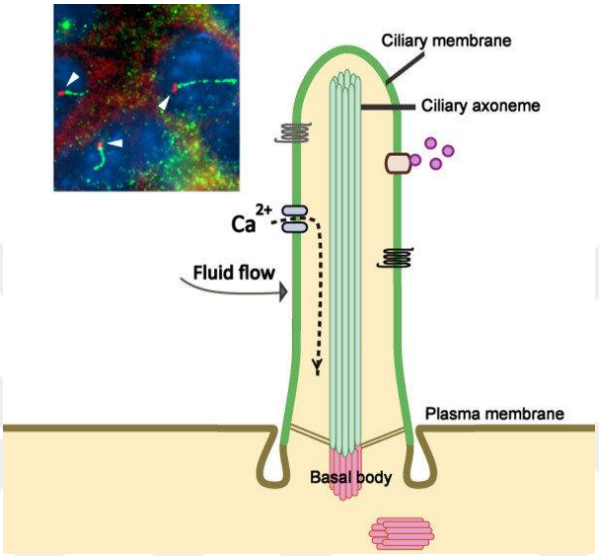

Figure 3: Primary cilia structure (Hsiao, Tuz and Ferland, 2012).

Primary cilia are involved in regulation cell growth, homeostasis, and development of tissues by coordinating signaling pathways such as Shh, Wnt, RTK, ECM receptors and calcium channels (Pedersen et al, 2016, Malicki and Johnson, 2017). It has been shown to play a role in preserving stem cell activity by signal transduction (Ritter et al, 2018). Primary signaling pathway controlled by primary cilia is Hedgehog whose receptors are found on the membrane of PC. Sonic hedgehog (Shh) is the main molecule to activate Hh pathway in PC. In the absence of Shh, Ptch1 receptor is situated on the ciliary membrane and blocks the entrance of SMO, signaling receptor, into to the cell. Different from canonical Hh signaling, Gpr161, a GPCR molecule, is also located on the ciliary membrane leading to amplification of cAMP production. This elevated level of cAMP causes the activation of PKA triggering the proteolytic cleavage of GLI transcription factors. In ON state of Hh signaling, Shh binding to Ptch1 initialize the clearance of both Ptch1 and Gpr161 receptors from ciliary membrane so that SMO enters the cell along with the Gpr175. Disappearance of GPCRs causes a decrease in cAMP level and promote stabilization of GLI and expression of target genes (Pedersen et al, 2016). Additional

to coordination of Hedgehog signaling, primary cilia membrane incorporates ciliary calcium channels to control Ca^{2+} concentration of cells. The change in the calcium concentration also influences modification of SMO and activation of GLI transcription factors Gli1 and Gli2 (Delling et al, 2013). Studies genetically target Ift88/ Kif3a genes which are major genes that contribute to the production and assembly of primary cilia in order to deplete PC and observe specific functions of them. When PC cannot be generated in ciliated cells, Shh signaling becomes nonfunctional and cells cannot respond to Shh ligand (Bangs and Anderson, 2017). One of the recent studies revealed the importance of primary cilia function on adipogenesis because PC acts as a sensor for growth factors and nutrients in the environment. Ciliated pre-adipocytes were found to contain omega 3 fatty acid receptors FFAR4/ GPR120 on the ciliary membrane to promote an increase in adipogenesis depending on the fatty acid composition in surrounding tissues. Further, PC depletion from such pre-adipocytes leads to decline in adipogenesis rate resulting in decreased fat mass of the body (Hilgendorf et al, 2019). Another pioneer study demonstrated the importance of PC on adipogenesis and how different environmental cues such as high fat diet can be sensed by ciliated cells. Ritter et al. revealed that adipose derived mesenchymal stem cells (ASCs) contain primary cilia involved in responding to environmental stimuli. They collected ASC samples from obese and lean individuals showing that primary cilia from obese ASCs were defective, shortened and not responsive to signals. Such nonfunctional primary cilia structures render stem cells deficient resulting in unhealthy adipose tissue. As mentioned, primary cilia are highly important for transduction of hedgehog signaling. Thus, primary cilia defects in obese ASCs result in impaired transport of signaling molecules such as SMO to the ciliary membrane leading to insufficient hedgehog signaling (Ritter et al, 2018). Considering the functions, primary cilia are vital organelles to assure coordination of cells depending on environmental stimuli in both homeostatic and disease states.

1.6 Disease and Dietary Animal Models

Under homeostatic conditions, resident microbial communities are found in interaction with mucosa on epithelial layer of small intestine and contributing to absorption of nutrients to an extent (Xavier and Podolsky,2007). Besides nutrition absorption, small intestine functions as a barrier and sensor against pathogens (Smilie et al, 2019).

1.6.1 High Fat Diet Induced Obesity Model

Small intestine is responsible for nutrient absorption so, intestinal stem cells are affected by any change in the dietary signals. They regulate generation of progenitor cells and daughter stem cell number to adapt new nutritional conditions. As shown by Ritter et al., obesity drastically affects adipogenesis and response toward environmental stimulus. These changes in responsive capacity of cells can also be observed in small intestinal function (Ritter et al,2018). A study to show effect of high fat diet on intestinal stem cell activity demonstrated that higher fat composition of diet cause shortening of small intestine and decrease in weight of tissue. By affecting the cell composition, mice fed with HFD have decreased number of enterocyte and change in the crypt villus architecture. Further, an increase in the expression of stem cell marker Olfm4 was observed as opposed to diminished population of Paneth cells. These results suggest the boosted regenerative capacity of intestinal stem cells as a response to high fat diet. Increased proliferation rate of stem cells despite the fewer Paneth cell number presents the notion of stem cells activity independent from epithelial niche factors. It can be speculated that these stem cell populations could benefit from alternative ligand sources of stem and progenitor cells in proximity (Beyaz et al,2016).

1.6.2 Western Diet Model

Similar to obesity, nutrient diversity and uptake levels are very crucial for regular functioning of intestinal and colonic stem cells. Colorectal cancer is reported to be most common form of disease and malignancy in Western populations (Fodde et al,2016; Chan et al,2010; Li et al,2019). Prolonged dietary habits of those populations containing higher fat, low vitamin D3 and low calcium levels are known to constitute the main risk factors for colon cancer (Peregrina et al,2015; Fodde et al,2016; Newmark et al,1990; Li et al,2019). Even though Western style diet doesn't result in obesity as opposed to high fat diet, these nutrient levels create a predisposition for tumorigenic state in both intestinal and colonic epithelium (Peregrina et al,2015). Mice models using Western diet are generated specifically to study intestinal cancer by providing similar levels of risk bearing nutrients such as lower vitamin D3 and lower calcium mimicking those individuals in Western populations (Li et al,2019). Recent studies show the relationship between Western style dietary habits with activity of stem cells of intestines. Upon long term administration of Western diet containing higher fat and lower vitamin D3, especially Lgr5+ crypt base columnar stem cells were observed to exhibit not only decreased activity but also reduction in number (Li et al,2019; Peregrina et al, 2015). Further, such nutrient levels create a pre-tumorigenic condition in colonic mucosa (Peregrina et al,2015). Thus, both

Western diet and high fat diet could be utilized to study intestinal stem cell function from different angles on a nutritional level.

1.6.3 Dextran Sodium Sulfate (DSS) Induced Colitis Model

Disease state disrupts the integrity of epithelium and the barrier function leading to inflammation in intestinal tissue resulted from invasion of such microorganisms. This disease condition is named as Inflammatory Bowel Disease (IBD) and it has two major form including Ulcerative Colitis and Crohn's Disease. Ulcerative colitis is mainly characterized by inflammation mucosal layer of intestine. As a result, inflammatory mediator production is increased along with the accumulation of large number of neutrophils in majorly lamina propria and crypt regions. Epithelial layer is mainly affected from the inflammation and severe injury in that layer is observed. In colitis case, Goblet cells rather than Paneth cells play a role both as safeguard against pathogens and in development of disease. On the other hand, Crohn's disease is defined with inflammation in transmural regions. It leads to macrophage accumulation at inflammation sites (Xavier and Podolsky,2007). During ulcerative colitis, both innate and adaptive immunity are involved for protection and clearance of pathogens thus, increase in expression of genes related to inflammation can be observed compared to healthy state (Smilie et al, 2019). Apart from pathogenic effects, changes in the expression of critical niche factor genes such as Noggin, R-spondin, BMP, Wnt can also provoke colitis development such that deregulation of these factors hinders the regenerative capacity of stem cells resulted in impaired wound healing. Dextran sulfate sodium (DSS) is a widely used chemical in experimental purposes to mimic ulcerative colitis in mouse models. A study on mesenchymal remodeling of small intestine in case of colitis showed that DSS treatment induces expression of mesenchymal cell markers due to depletion of mesenchymal niche factors. Because epithelial layer and mesenchymal niche are disrupted, stromal remodeling is required to regenerate the damaged tissue. Also, it is observed that stem cell marker Lgr5 expression possibly promotes repair and regeneration of damaged tissues (Kinchen et al, 2018). Even though effects of colitis on epithelial layer and mesenchymal niche were explored, how intestinal cell types are responsible for regeneration of stem cells and niche are remains unknown. Revealing the mechanism behind this recovery process and reconstitution of stemness and niche factors constitutes a remarkable question waiting to be solved.

2. OBJECTIVES AND AIMS

In this thesis project, we aimed to characterize enteric nervous system subpopulations and whether those detected populations are altered when homeostatic state is disrupted along with the ciliated cell populations in small intestine and colon. It was known that ENS is involved in the vital functions of intestinal functioning however, its specific cell composition and their involvement in damaged tissue have not been studied extensively up to date. Also, primary cilia were known to be expressed in intestinal tissue, yet which specific cell types possess this organelle has not been described. Further, ACOT7 protein was shown to have an important role in fatty acid hydrolysis in neurons in brain. Upon reanalysis of single cell RNA sequencing data of a recent publication on colitis model, we selected ACOT7 for further analysis in small intestine and colon to detect responding ciliated cells.

After observing ACOT7 to specifically mark ganglia containing ENS cells, we hypothesized that those ganglionic regions in the myenteric and submucosal plexuses could have a functional role in disease models including colitis and obesity.

In order to assess our hypothesis, our aims were to:

1. Describe neuronal and glial cell populations that generate ACOT7 expressing ganglionic structures. This goal will provide us with detailed information on the cell network and composition of those ENS cells along with defining an ENS marker for ganglion composition globally or specifically for various cell types. For this purpose, we selected HuCD, Tuj1 and PHOX2B as neuronal markers while S100beta was selected as a glial cell marker.
2. Understand how ENS cells are involved in metabolic diseases and inflammation in small intestine and colon. Because ENS has not been studied extensively, with this purpose, we aimed to achieve an alternative component to contribute to intestinal tissue preservation upon damage rather than stem cells and their niche.
3. Identify ciliated cell populations in several intestinal tissue layers including mesenchymal, myenteric plexus and submucosal plexus. With this goal, we sought to define a distinct mesenchymal niche subcluster supporting stem cells involving in the signal transduction. To achieve our goals, we used Arl13b protein as a marker for primary cilia axonomes and PCNT as a marker for primary cilia base.

4. Define whether those ENS and mesenchymal subpopulations are interacting with each other in response to disease conditions. Thus, we used specifically PDGFRA as a well-studied mesenchymal cell type.
5. Reveal insights on communication along gut-brain axis when an inflammatory state is appeared on colonic epithelium. With this specific aim, we were focused on whether this interaction of neurons and glial cells with PDGFRA+ cells were prominent in the brain. To be able to assess this, we used same ENS markers in brain as well.

Thus, in this thesis, we developed high fat diet induced obesity and DSS induced colitis mouse models to reach our goals. We conducted series of IHC and imaging analysis with aforementioned markers in small intestines, colons and brains of those model animals.

3. MATERIALS AND METHODS

3.1 Animal Model Generation

All animals were housed in Animal Facility of Bilkent University (Ankara, Turkey). All procedures were carried out in accordance with an approval of the Ethical Committee of Bilkent University. High fat diet induced obesity model was generated by using 8-12 weeks old gender matched C57BL/6 strain mice (n=37). They were fed with 60 kcal% fat composed diet (Research Diets, NJ, USA, D12492) *ad libitum* for up to 24 weeks. Control groups (n=42) were fed with regular chow diet (Optima, Bolu, Turkey) *ad libitum* duration matching the experimental group. The weights of mice were measured every two weeks. A number of mice from both experimental and control groups were excluded from the setup due to health and compatibility issues.

Western diet model was generated by using 8-12 weeks old gender matched C57BL/6 strain mice (n=25). They were fed with 40 kcal% fat and 20% protein composed diet (Research Diets, NJ, USA, D12079B) *ad libitum* for up to 24 weeks. Control groups (n=25) were fed with regular chow diet (Optima, Bolu, Turkey) *ad libitum* duration matching the experimental group. The weights of mice were measured every two weeks.

Dextran sodium sulfate (DSS) induced colitis model was generated by using 8-12 weeks old C57BL/6 mice (n=12). Their autoclaved drinking water was supplied with 2.5% DSS (MP Biomedicals, CA, USA, 02160110) for 5 days *ad libitum*. At the end of day 5, their DSS supplied water was changed to regular drinking water to allow recovery for 2 days. The control group was supplied with regular autoclaved drinking water for 7 days *ad libitum* (n=6). The weights of the animals were measured at the beginning of each time point.

3.2 Intestinal and Cerebral Tissue Isolation

Small intestine and colon tissues were collected from all three experimental setups. Mice were euthanized using isoflurane. After midline laparotomy, cardiac perfusion with 4% paraformaldehyde (PFA) (Fluka) in PBS or 10 % formalin solution (Sigma Aldrich, MO, USA, HT501128) was performed. Small intestine tissue was collected from duodenum to ileum. Cecum was discarded. Colon tissue was collected from cecum until anus covering proximal and distal regions. After collection of tissue, they were flushed with ice cold 1X PBS and they were cut into around 1 cm pieces. They were washed with 1X PBS for 2 times for 5 minutes each. They were fixed with 4 % PFA. Tissues that will be embedded in paraffin were fixed overnight

at +4℃ while tissues that will be embedded in O.C.T were fixed for an hour on ice. For paraffin embedding, tissues were washed and dehydrated by using 30% EtOH/PBS and 50% EtOH/ ddH_2O for an hour each at room temperature. Tissues were prepared in cassettes in 70% EtOH for tissue processing. An automated tissue processor was used. Tissues were embedded in paraffin longitudinally and transverse. For frozen block preparation, after fixing with 4% PFA, tissues were washed and incubated in 30% sucrose (Fisher Chemicals, NH, USA, 10634932) overnight at + 4℃. Afterwards, they were embedded in Tissue-Tek O.C.T Compound (Sakura Finetek, Tokyo, Japan, 4583) longitudinally.

Cerebral tissues were isolated from DSS induced colitis model animals. Same autopsy procedures were followed. After isolation of whole brains, they were quick washed with 1X PBS and fixed with 10% formalin solution for an hour on ice. After fixation, they were kept in 10% sucrose for 2 hours at + 4℃ followed by overnight incubation in 20 % sucrose. Followingly, they were further incubated in 30 % sucrose overnight at + 4℃. They were embedded in Tissue-Tek O.C.T Compound horizontally.

3.3 Immunohistochemistry

Paraffin embedded tissues were cut in 5 µm sections using a microtome. Sections were deparaffinized in Xylol for 15 minutes. They were dehydrated by using 100%, 96%, 80%, 70% and 50% EtOH. They were washed with 1X PBS 3 times for 5 minutes. Antigen retrieval step was carried out in a steam cooker (Tefal, France) either with citrate buffer (pH 6.0) or Tris-EDTA buffer (10 mM Trizma base, 1 mM EDTA, pH 9.0) for 35 minutes. After tissues were cooled down, they were blocked with blocking buffer including donkey serum (Biowest, MO, USA), 10X PBS and 0.3 % TritonX100 detergent in PBS (PBS-T). Afterwards, they were subjected to primary antibody incubation with respected markers (Appendix IV) overnight at + 4℃. After washing, secondary antibody staining (Appendix IV) was carried out for an hour at room temperature. Several steps of washing were carried out with PBS and 0.03 % PBS-T. Slides were stained with DAPI diluted in PBS-T for 10 minutes and washed. They were mounted with coverslips by using mounting medium (Abcam, Cambridge, UK). Slides were stored at + 4℃.

O.C.T embedded tissues were cut in 10 µm sections using cryostat. Sections were fixed in respective fixative agent for 10 minutes. After washing, they were incubated with blocking buffer. Staining steps were followed as described above. For brain sections, the only difference

was the lack of fixation steps of cut tissues. Antigen retrieval step for frozen sections were carried out depending on the primary antibody (Appendix IV).

3.4 Confocal Microscopy Analysis

Images were acquired using a Leica TCS SP8 DMI8 Confocal Microscope (Leica Biosystems, Wetzlar, Germany). For small intestine and colon, images were mainly focused on the myenteric plexus layer and crypt bottoms. For brain, images were taken from thalamus and insular cortex. Images were taken in 20X, 40X and 63X magnifications respective to the staining. Z-stacks were selected with a range of 10-40 stacks depending on the region and magnification. Obtained images were processed by using Fiji (Image J).

4. RESULTS

In this thesis, we investigated the response of small intestine and colon under certain metabolic conditions such as obesity and colitis. Epihelium, supporting mesenchymal layer and enteric nervous system were the main focus of the study. To unravel the underlying involvement of such cells interplay, we conducted a series of immunohistochemistry analysis on several mouse models.

4.1 Intestinal Cell Markers in Obesity

Intestinal tissues involve in the fat metabolism and reabsorption of food and water. Thus, the alterations in the stem cell activity and epithelial rearrangement have been studied in the previous years.

4.1.1 Intestinal Proliferative Cells in Obesity

To observe how proliferative cells respond to obesity conditions in the intestine, we checked for Ki67 expression by IHC staining. In both small intestine and colon, we saw that Ki67+ proliferative cells at the bottom of crypts increase their activity upon 24 weeks high fat diet administration when compared to controls (Figure 4A-D). Further, we observed that length of the small intestine (from duodenum to ileum) and colon were shorter in obese animals than control tissues (data not shown). Even though size of the crypts and length of the villus of small intestine from obese mice were not affected (Figure 4A-B), colonic crypts become shorter in obese mice (Figure 4C-D).

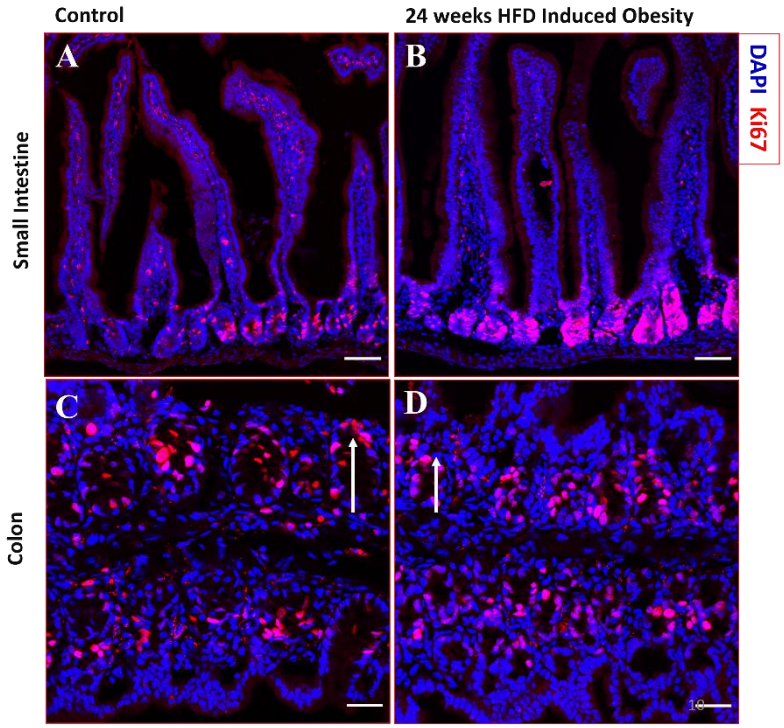

Figure 4: Proliferative cells shown by Ki67 (red) IHC stainings. Ki67+ cells can be observed at the crypt of small intestine of control (A) and 24 weeks HFD diet induced obese animals (B). Colonic crypts also shows Ki67 expression in control (C) and obese (D) animals. Scale bar represents 50 μm.

4.1.2 Intestinal Epithelial and Stem Cell Response to Obesity

After checking the proliferative cells' reaction to high fat diet, we wanted to analyze whether known mesenchymal subpopulation which is composed CD34+ cells responds to obesity induction. CD34 is expressed in intestinal submucosal plexus layer in addition to mesenchymal cells in close proximity to crypts (Figure 5A, 6A). In obese animals, the expression was observed to be diminished and the localization of signal was more prominent in the submucosal layer in both colonic and small intestinal crypts (Figure 5B,6B). Because it was suggested in previous studies that stem cell and niche activity were affected upon obesity, we wanted to investigate the Paneth cell activity change in experimental animals. To specifically detect Paneth cells in the small intestinal crypt base, we used lysozyme antibody for IHC analysis. We observed that there is no significant change in the expression level or the number of Paneth cells in obese animals compared to controls (Figure 5C-D).

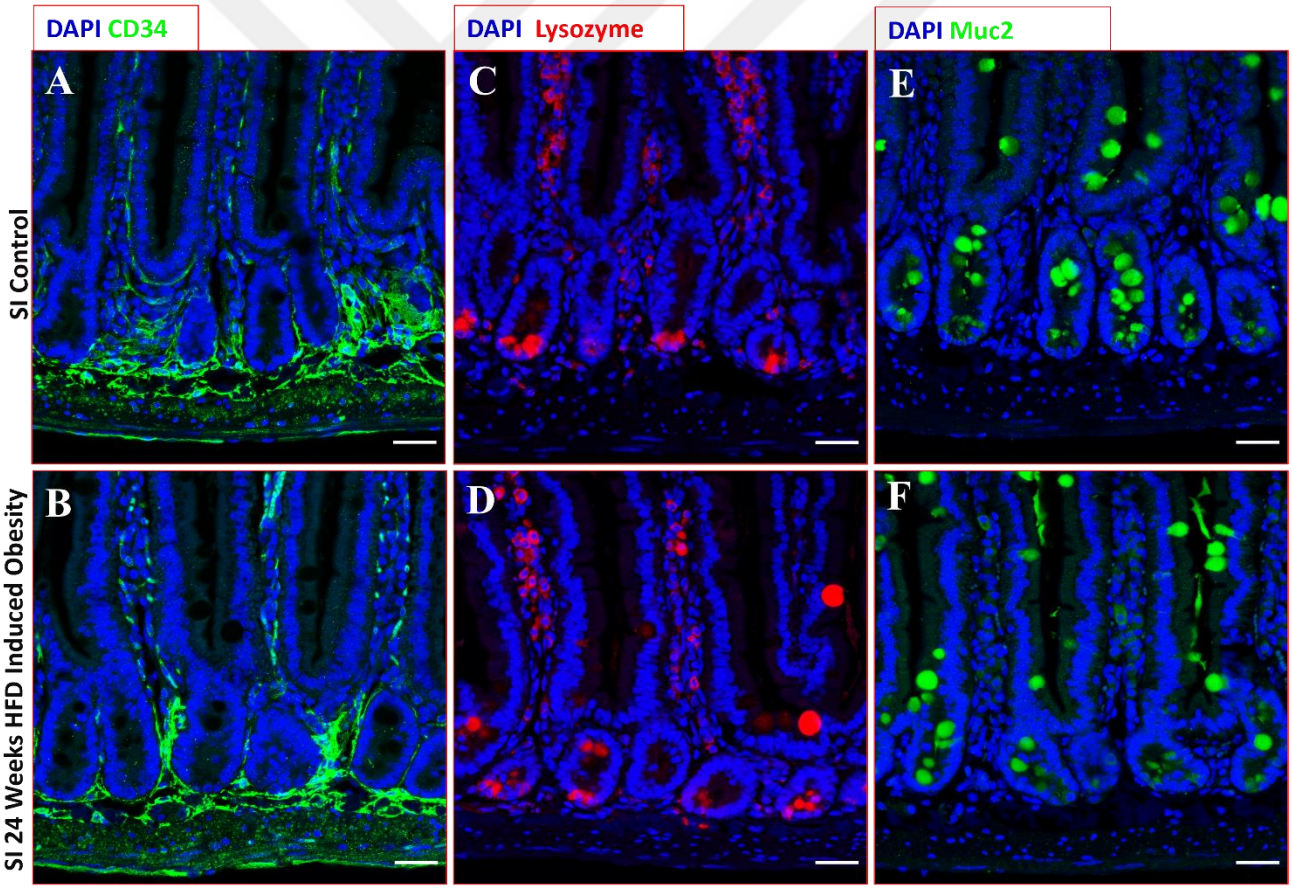

Figure 5: Small intestine IHC analysis of CD34+ mesenchymal cells (green,A,B), lysozyme+ Paneth cells (red,C,D) and Muc2+ Goblet cells (green, E,F) in control and obese mice (n=2). Scale bar represents 50 μm.

Apart from Paneth cells, epithelial layer is composed of large quantity of enteroendocrine cells which are mainly constituted by Goblet cells. This composition is more prominent in colonic

epithelia rather than small intestine. Muc2 is a very common marker to mark Goblet cells in tissues. So, we observed that in small intestine, there is no visible change in expression of Muc2 or number of Goblet cells in obese animals whereas there is a reduction in expression level of Muc2 in colonic crypts (Figure 5E-F, 6C-D). Further, even though we didn't observe critical alterations of those epithelial cells in small intestine, we saw some misdifferentiated cell types in secretory lineage. IHC stainings of obese animals showed lysozyme expression in some of the Goblet cells (Figure 5D) while Muc2 was observed to be expressed in some other enteroendocrine cell types which don't resemble Goblet cells phenotypically (Figure 5F).

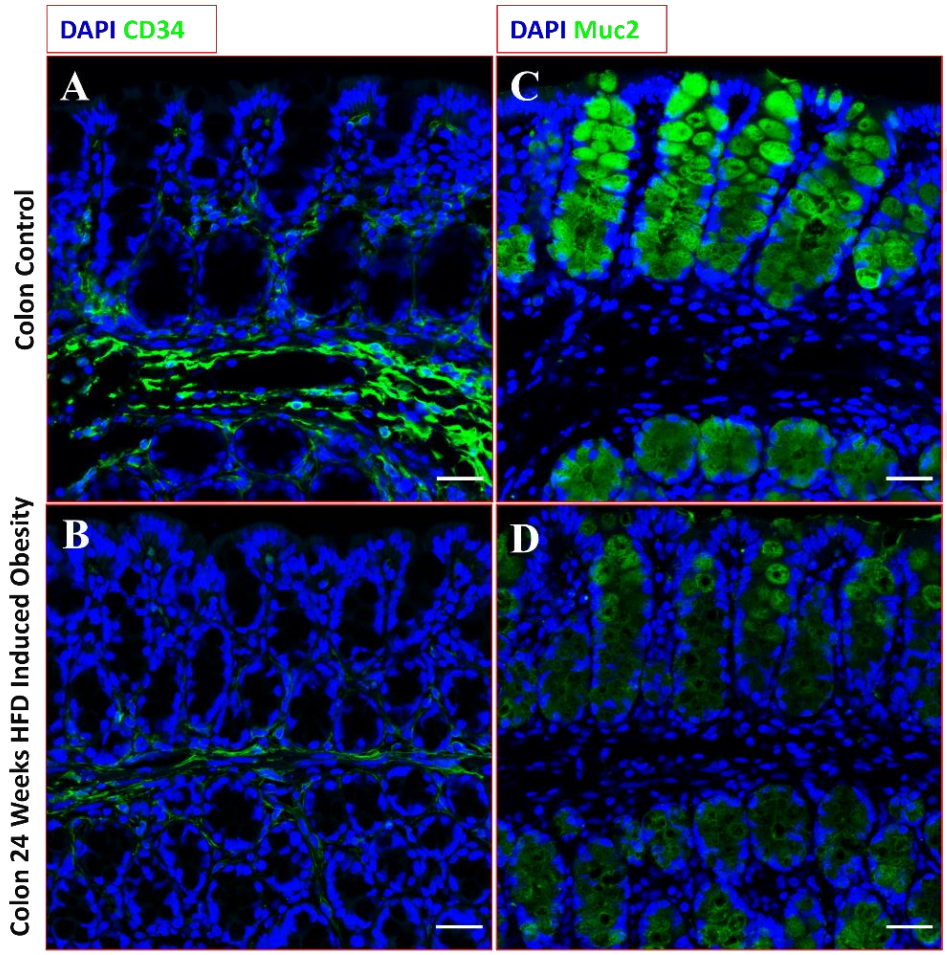

Figure 6: Colon IHC analysis of CD34+ mesenchymal cells (green,A,B) and Muc2+ Goblet cells (green, C,D) in control and obese mice (n=2). Scale bar represents 50 µm.

In line with the previous findings suggesting an increase in stem cell activation upon long term high fat diet administration, we used Olfm4 which specifically marks CBC cells and Sox9 being a transciption factor regulating stemness and Paneth cell activation in small intestine. We didn't observe any significant change in both Olfm4 and Sox9 expression levels in obesity models compared to controls (Figure 7A-D). Interestingly, we found Sox9 expression in some cells of myenteric plexus layer in both control and obesity (Figure 7C-D).

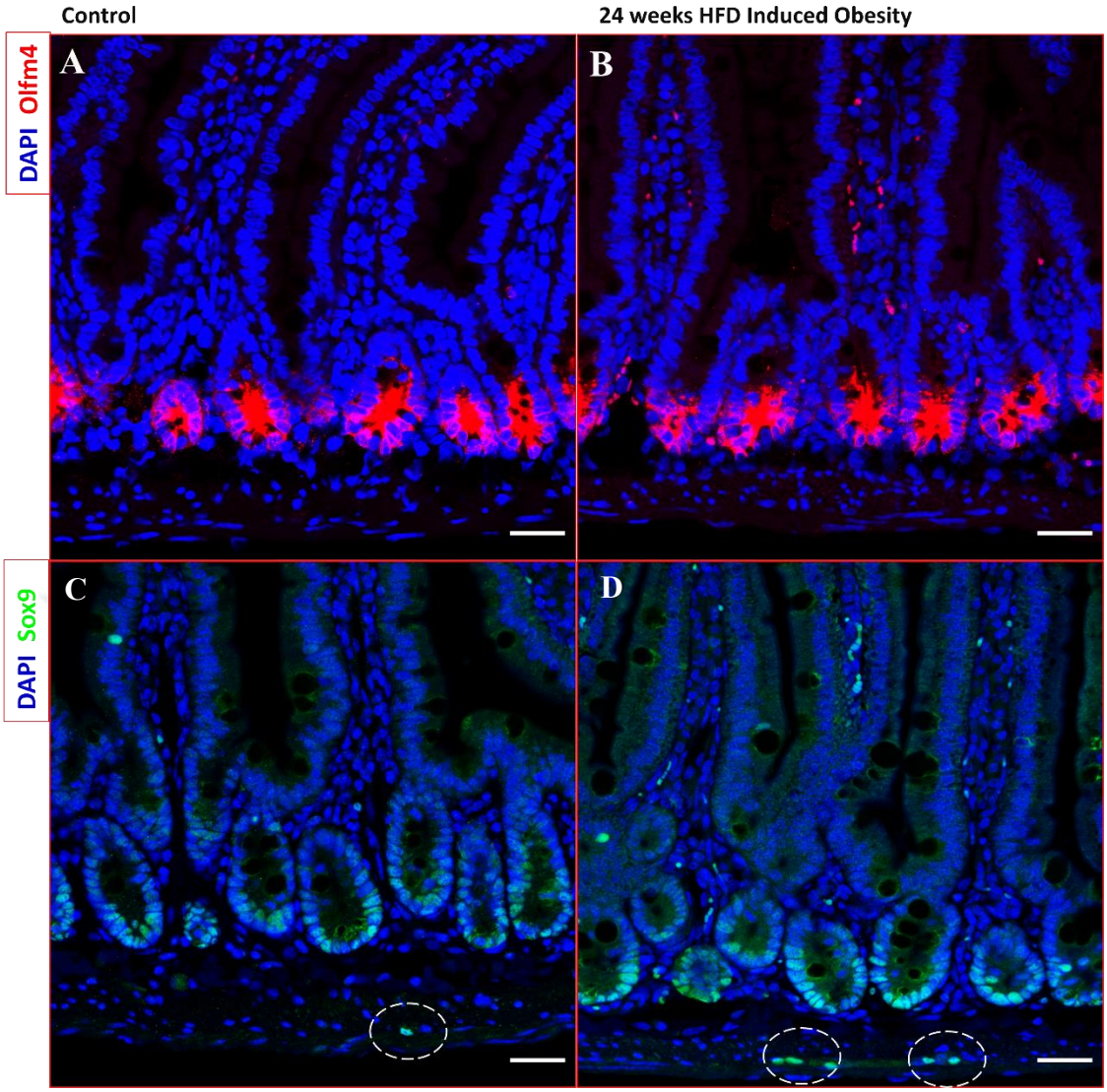

Figure 7: IHC stainings showing Olfm4+ (red) and Sox9+ (green) cells in small intestine. Olfm4 expression is detected at the bottom of the crypt in control (A) and obese (B) animals. Sox9 was observed in both intestinal crypst and myenteric plexus (dashed circles) layer of control (C) and obese animals (D). Scale bar represents 50 μm.

4.1.3 Intestinal Extraepithelial Niche in Obesity

Extraepithelial cells support stem cell activity by providing ligands and some other factors. Even though these mesenchymal subpopulations are heterogenous, there are some defined cell types known to have a crucial role in small intestine and colon. One of the distinct cell populations is CD34+ cells which were previously described in section 4.1.2. In this chapter, the mesenchymal ciliated cells that we described will be the focus.

4.1.3.1 Identification of Primary Cilia in Intestine

In order to identify localization of ciliated cells in the intestinal tissues, we used Arl13b (ADP-ribosylation factor like protein 13B) to specifically mark axonome of the primary cilia. Pericentrin (PCNT) which functions as an anchor for cilia was used to detect point of origin of primary cilia in those cells to be able to verify Arl13b signal (Figure 8A,D). Ciliated cells were shown to be localized in the lamina propria and mesenchymal layer in very close proximity to crypts (Figure 8B,E). Further, primary cilia are observed to be located in the myenteric plexus and submucosal plexus layers (Figure 8C,F).

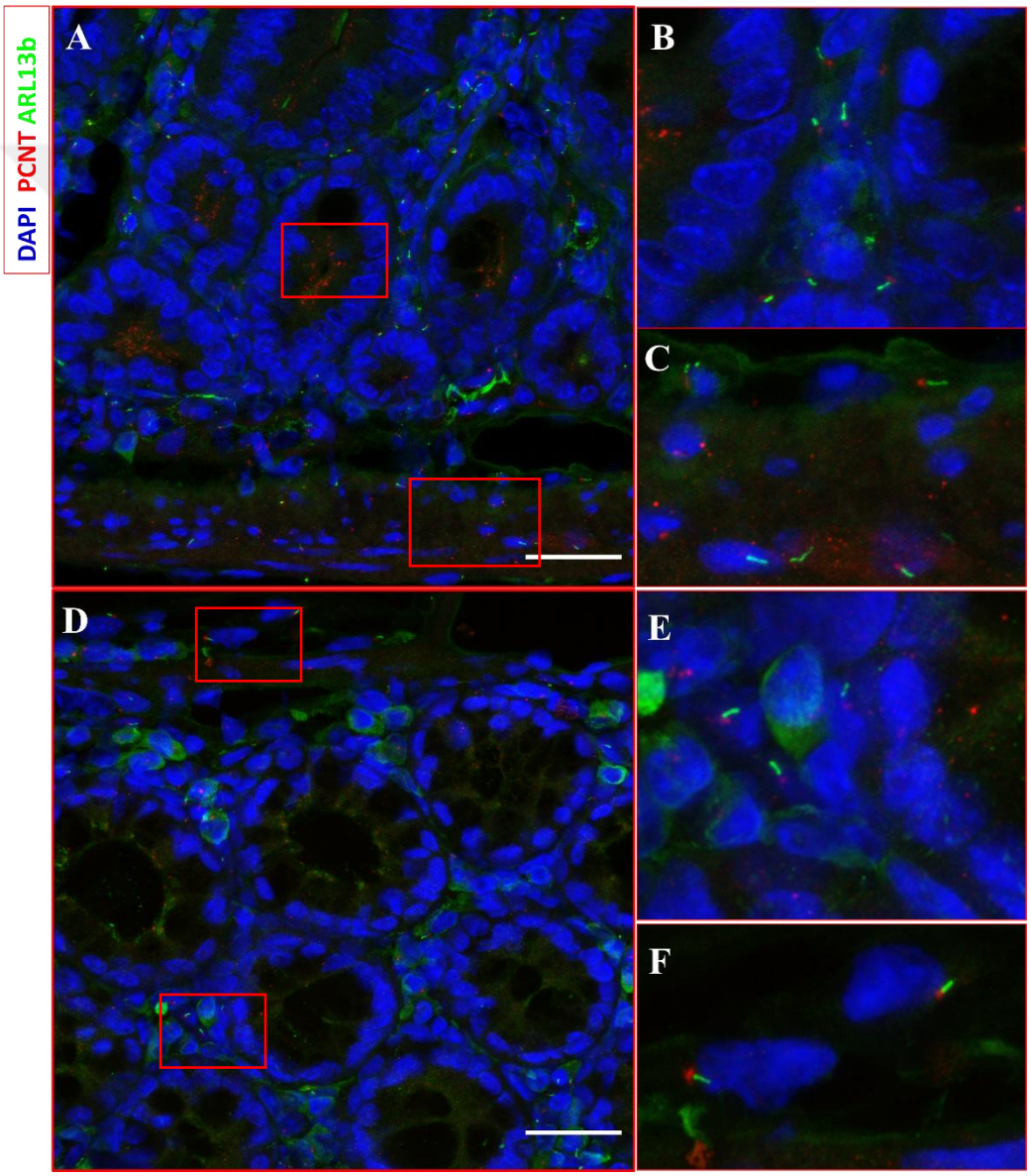

Figure 8: Small intestine IHC staining against primary cilia (Arl13b green and PCNT red,A). Ciliated cells are located in mesenchymal layer (B) and in myenteric plexus layer (C). Similar localization can be observed in colonic mesenchyme (E) and submucosal plexus (F). Scale bar represents 50 μm.

4.1.3.2 Ciliated Cell Response to Obesity in Intestine

To further investigate the primary cilia in the disease state, we checked for Arl13b expression under obesity condition. Similar localization was observed in both control and obese animals. Primary cilia were expressed strictly in the mesenchymal layer and not in the epithelial layer differentiated by using PDGFRA and E-cadherin respectively (Figure 9A-D). PDGFRA+ cells were found to be co-expressed with a primary cilium. Primary cilia are found in great numbers heterogeneously dispersed along the whole tissue mesenchyme and plexuses. Because of that, we didn't observe any significant change in the number of cilia expression in obese animals compared to control (Figure 9A, B). After generating obesity model, we wanted to confirm whether our data is resulted from obesity condition rather than the content of the diet. Thus, we used Western diet model for same period of time, 24 weeks administration. Even though Western diet has also higher fat content compared to chow diet and experimental mice gained substantial weight, they cannot be classified as obese animals. We observed that primary cilia number was not affected by Western diet administration in both small intestine and colon compared to controls (Appendix VI).

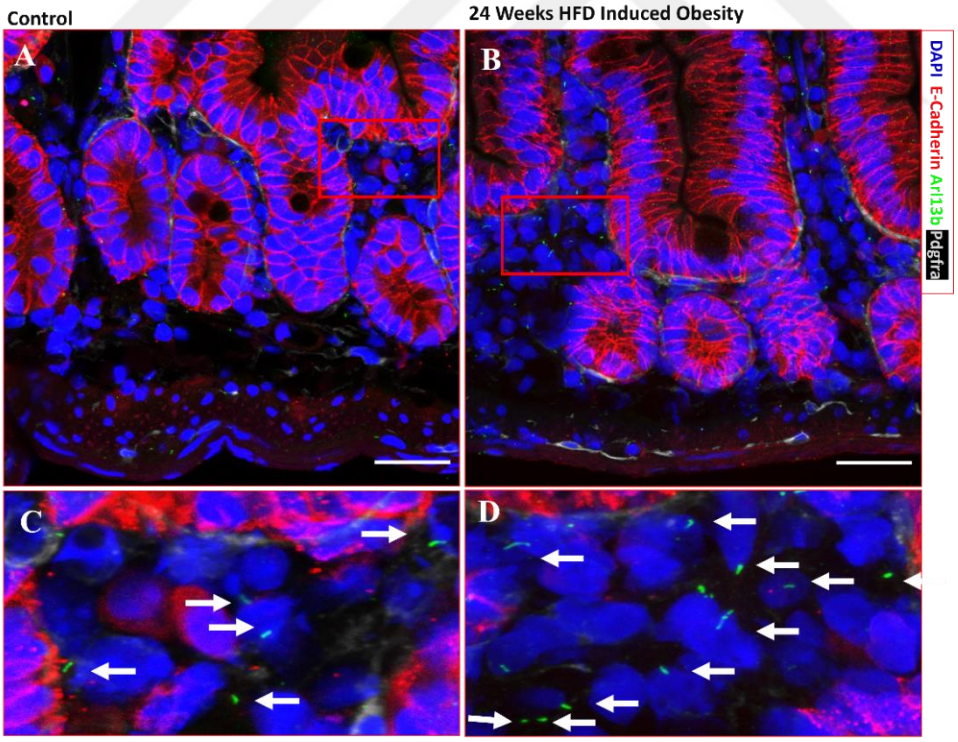

Figure 9: IHC stainings against ciliated cells in small intestinal mesenchyme marked by Arl13b (green), epithelial cells by E-cadherin (red) and mesenchymal cells by PDGFRA+(gray) in control (A) and obese (B) animals. C and D panels shows zoom in images of indicated mesenchymal regions. Arrows Show Arl13b+ primary cilia. Scale bar represents 50 μm.

4.2 Enteric Nervous System Activity in Intestine

Through re-analysis of single cell RNA-sequencing data from several previously published studies, we wanted to identify a differentially expressed marker that distinguishes primary cilia positive subpopulations in intestine. As a result, we decided ACOT7 protein could be used for this specific purpose (Smilie et al,2019).

4.2.1 ACOT7 as a Marker for Enteric Nervous System Populations

After further IHC analysis with ACOT7 antibody, we identified that it is distinctly expressed in submucosal plexus and myenteric ganglia (Figure 10A). By using E-cadherin staining, we showed that ACOT7 is also expressed in the Tuft cells in the epithelial layer of small intestine (Figure 10B). We confirm these ACOT7+ enterocytes to be Tuft cells by using αAcetylated Tubulin expression (data not shown). Interestingly, ACOT7+ ganglia in the myenteric plexus layer were observed to be tightly surrounded by PDGFRA+ cells (Figure 10C).

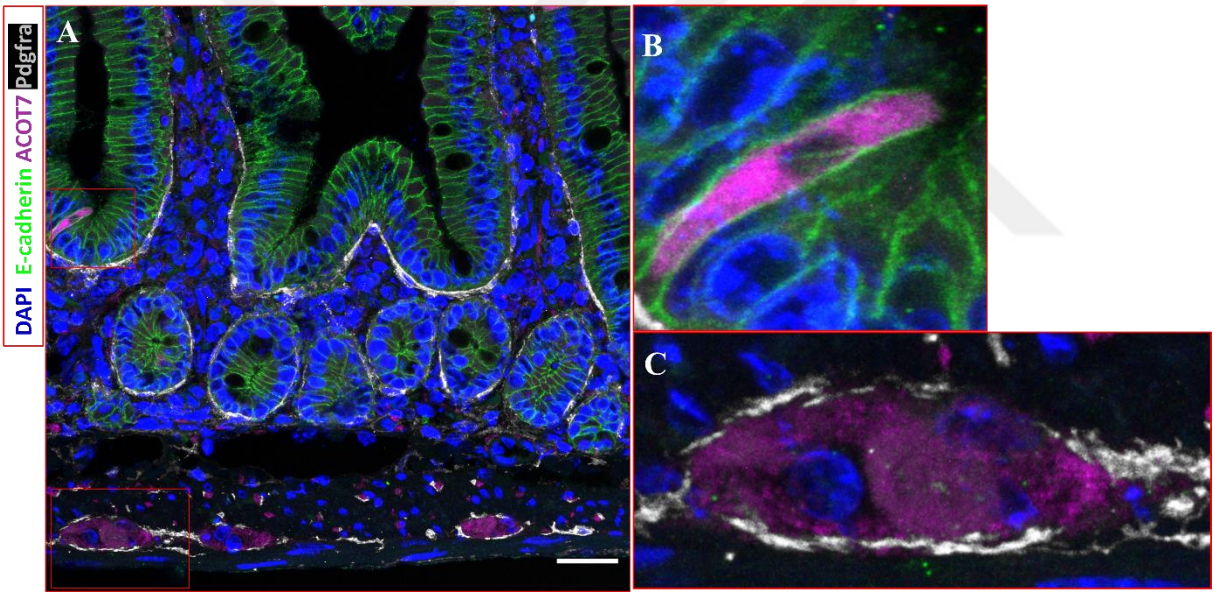

Figure 10: IHC analysis against ACOT7 (magenta)(A). Epithelial cells are marked by E-cadherin (green) and mesenchymal cells are marked by PDGFRA. ACOT7 specifically detects myenteric ganglion cells in the myenteric plexus(C) while it labels Tuft cells (B) in the epithelium as well. Scale bar represents 50 μm.

In small intestine, αSMA is expressed in the muscle layer and as an extension through the lamina propria. Co-staining it with ACOT7 showed that ACOT7+ ganglia in the myenteric plexus layer are found to be embedded in the muscle layer while they are negative for αSMA. Thus we can confirm that ACOT7 as a marker for ganglia rather than other extraepithelial subpopulation found the muscle layer (Figure 11A). In obesity condition, we didn't observe

any change in the co-localization of both proteins and in the expression level of αSMA (Figure 11B).

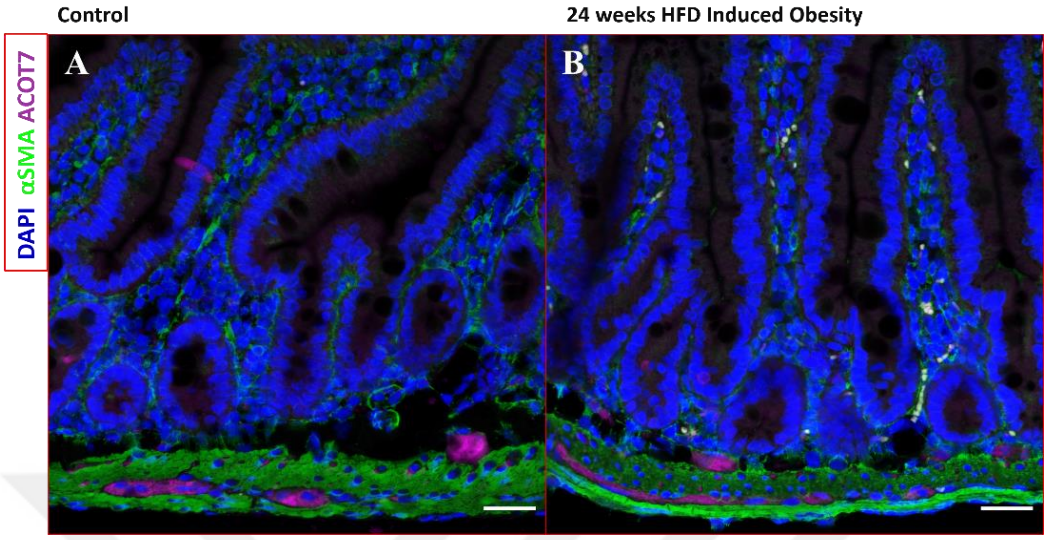

Figure 11: Small intestine IHC stainings against αSMA (green) and ACOT7 (magenta) in myenteric and submucosal plexus layers of control (A) and obese (B) mice (n=2). Scale bar represents 50 µm.

4.2.2 ACOT7 and Primary Cilia Co-expression in Obesity Model

After defining ACOT7 expression and ciliated cells in intestine, we further wanted to show whether those ganglia cells have primary cilia. Thus, we used IHC stainings against Arl13b and ACOT7 in small intestine. ACOT7+ cells in the myenteric plexus and submucosal plexus layers were observed to bear primary cilia structures in both control and obesity animals (Figure 12A-C).

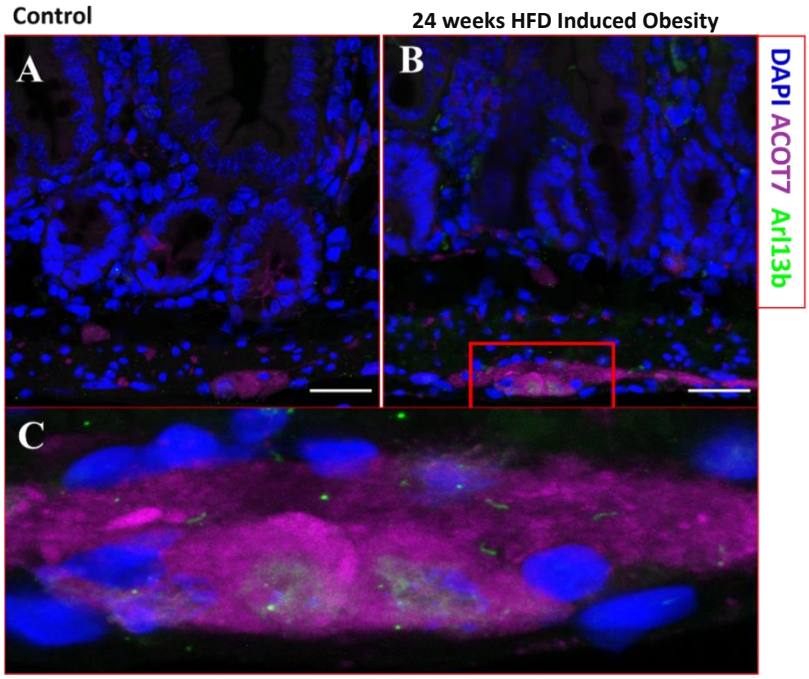

Figure 12: Small intestinal IHC analysis for Arl13b (green) and ACOT7 (magenta) in control (A) and obese (B) animals. Zoom in panel shows the primary cilia colocalization in myenteric ganglion with ACOT7 (C). Scale bar represents 50 µm.

4.2.3 Glial and Neuronal Cells in Obesity

In order to futher characterize ACOT7+ ganglionic cell subpopulations, we used HuCD as a common marker for nerve cell bodies and PHOX2B to detect neuronal and some glial cell nuclei in both small intestine and colon. ACOT7 was observed to be co-localized with both HuCD and PHOX2B (Figure 13A-D). Although these markers appear to be co-expressed in myenteric and submucosal cells, ACOT7 stains the ganglia as a whole including their extensions whereas, PHOX2B and HuCD specifically stains the nerve bodies. Additionally, HuCD signals cannot be observed in the absence of ACOT7 suggesting that ACOT7 distincly detects ganglia in a global manner in intestinal tissues. In obese animals, expression leve of HuCD and PHOX2B didn't change in parallel with ACOT7 response mentioned previously such that neurons cannot be found independently from ACOT7 expression (Figure 13B,D). As described above, upon high fat diet induction, colonic crypts were decreased in length while small intestinal structure was not affected (Figure 13C-D).

After confirming ACOT7 as a myenteric and submucosal ganglia marker for intestines, we wanted to specify functions and subpopulations of those ganglia. Thus, we carried out IHC stainings against Beta catenin which is a crucial component for Wnt signalling activation. We observed an overlap in ACOT7 and Beta catenin expression comprehending the whole myenteric plexus layer (Figure 14A-D). We didn't detect any change in the expression level of beta catenin and ACOT7 or structural alterations in ganglia (Figure 14B,D).

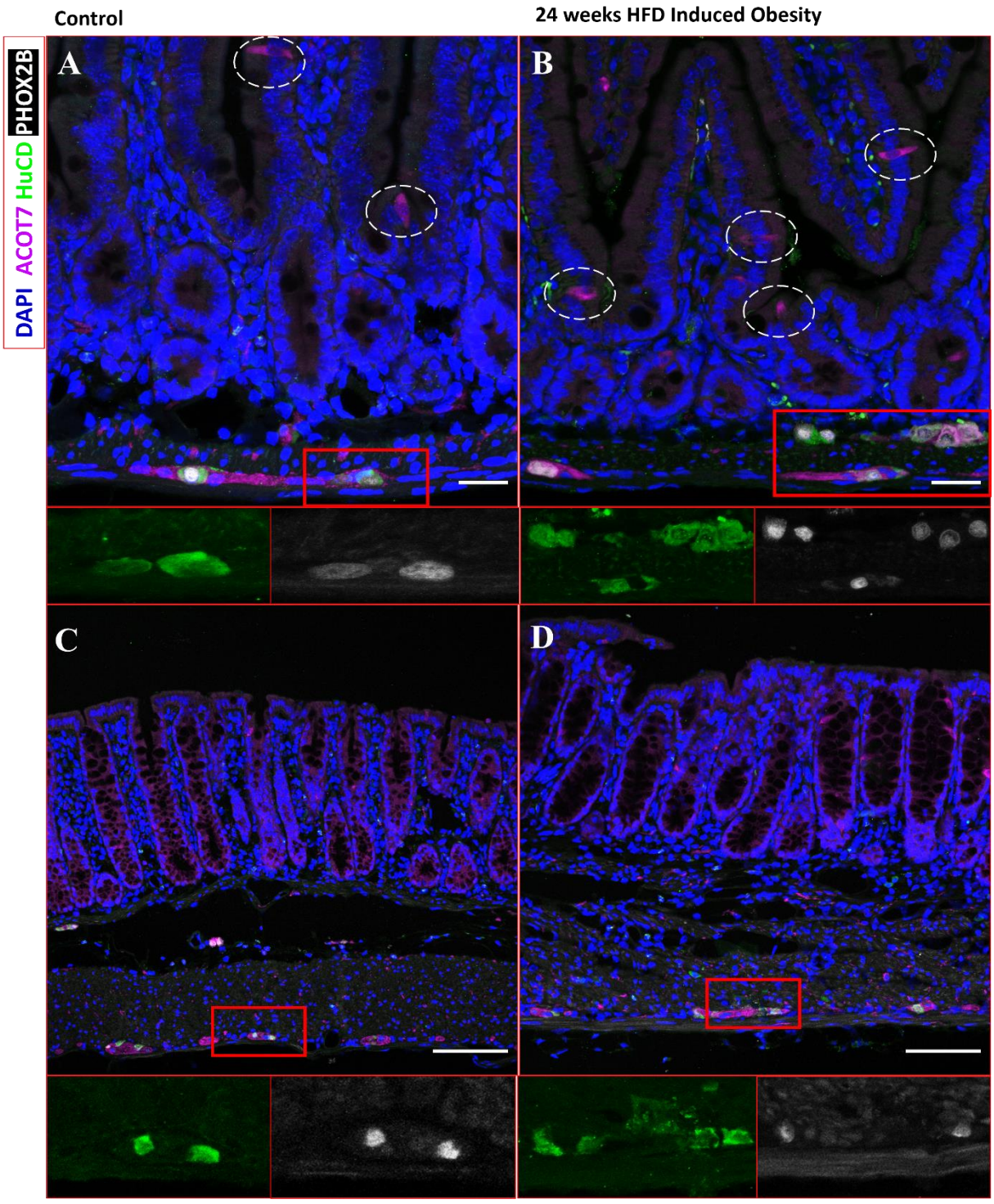

Figure 13: Intestinal IHC analysis of ACOT7+ cells of myenteric ganglia (ACOT7,magenta). ACOT7+ ganglion cells are co-localized with neurons cells marked by HuCD (green) and PHOX2B (gray). Small intestine control (A) and obese (B) animals and colon from control (C) and obese (D) animals show expression pattern in myenteric plexus and submucosal plexus. ACOT7 specifically marks Tuft cells in epithlelial layer (dashed circle). Scale bar represents 50 µm (A and B), 150 µm (C and D).

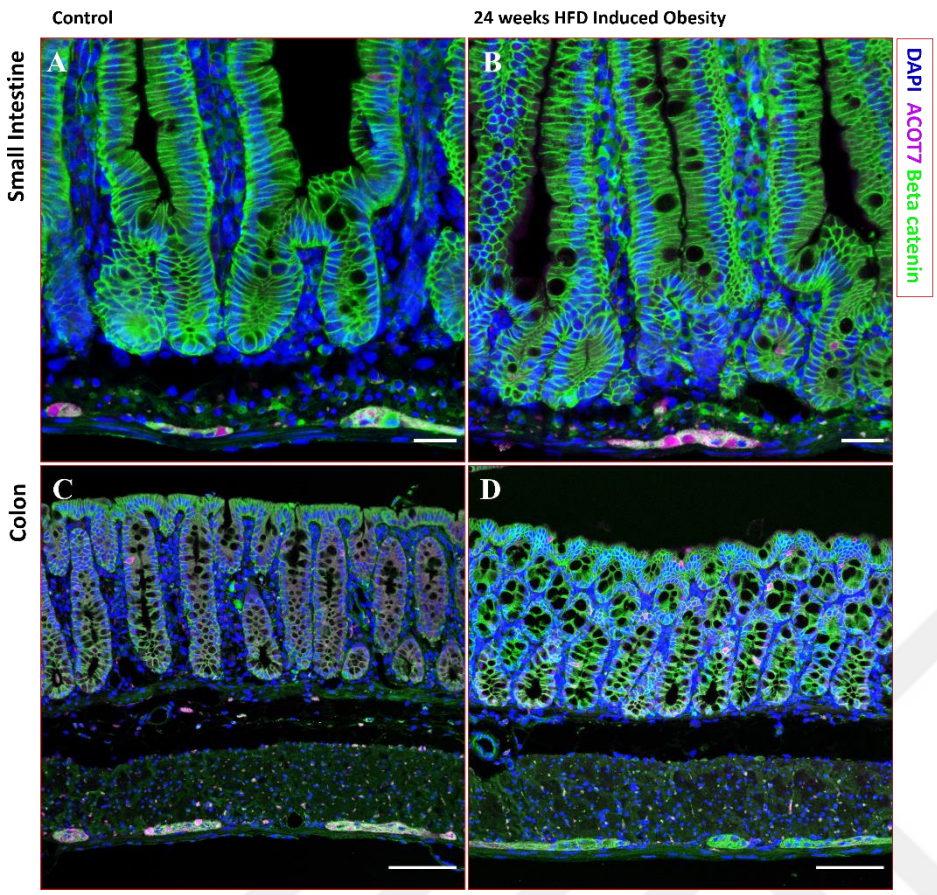

Figure 14: IHC stainings showing ACOT7 (magenta) and β catenin (green) expression located in small intestinal myenteric ganglion of control (A) and obese (B) animals. They were similarly co-localized in colonic myenteric plexus of control (C) and obese (D) animals. Scale bar represents 50 μm for A and B,150 μm for C and D.

As previously described, primary cilia were found to be located in the myenteric plexus layer apart from mesenchymal cells. Also, we showed that PDGFRA+ cells in the myenteric plexus layer define the regions for ACOT7+ neuronal ganglia. Thus, in order to further characterize subpopulations of ciliated cells, IHC analysis were carried out by using HuCD to detect neurons and PDGFRA to be able to differentiate myenteric ganglia. As a result, we observed a heterogenous distribution of ciliated cells along the myenteric plexus layer in both small intestine and colon (Figure 15A,C). Inside the ganglia encapsulated by PDGFRA expression, primary cilia were found to be expressed by HuCD+ cells whereas PDGFRA was observed to be co-localized with Arl13b in the border of ganglionic regions. Also, ciliated cells were found to be located in ganglionic and extraganglionic sites by being double negative for both HuCD and PDGFRA. When obese animals were investigated, they yielded similar distribution pattern for ciliated cells (Figure 15B,D). However, we observed a pattern of expression of PDGFRA in myenteric plexus layer more prominently in colon. In case of obesity, its expression was observed to be elongated towards the submucosal layer generating a vertical pattern (Figure 15D).

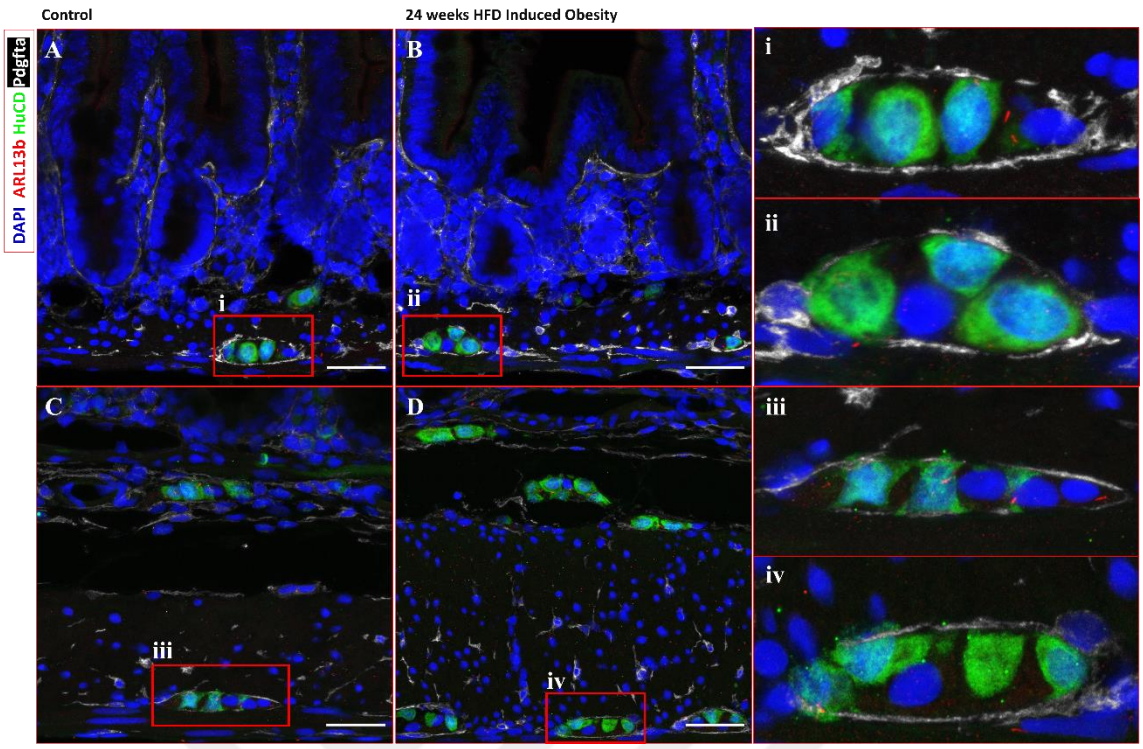

Figure 15: Small intestine (A,B) and colon (C,D) IHC analysis showing primary cilia (Arl13b,red) with neurons (HuCD,green) and PDGFRA+ cells (gray). Zooms Show primary cilia and neuron localization in myenteric plexus of small intestine (i,ii) and colon (iii,iv). DAPI was used to counterstain nucleus. Scale bar represents 50 µm.

To further evaluate the response of different subpopulation inside the intestinal ganglia, another commonly used specific marker for neurons was used. Tuj1 (beta tubulin III) detects neuron fibers. As expected, Tuj1 is expressed in both submucosal and myenteric plexuses of small intestine (Figure 16A) because it was previously described by HuCD expression that neurons are one of the subpopulations in the ganglia. Interestingly, neuron fibers stained by Tuj1 can be observed around the crypts elongating through the villi inside the mucosal layer different than the pattern we observed with HuCD and PHOX2B where they were strictly expressed in myenteric and submucosal plexuses (Figure 16A-B). When we examined the Tuj1 expression in obese animals, we didn't observe any difference compared to control in situ.

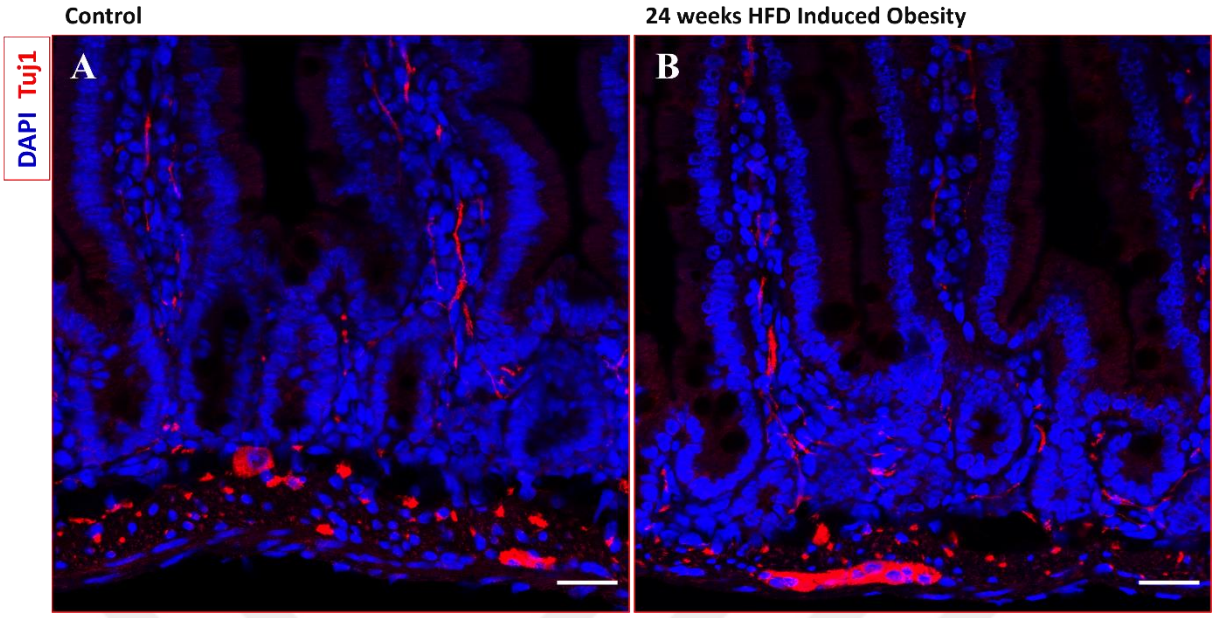

Figure 16: Small intestine IHC analysis for Tuj1 (beta Tubulin III,red). Neuron fibers are detected in the myenteric plexus, submucosal layer and in the lamina propria region of small intestine of wild type (n=2) mice (A) and high fat diet induced obesity model (B) (n=2). Scale bar represents 50 μm.

There are two main cell types in myenteric ganglia; neurons and glial cells. After detecting ACOT7 and neuron colocalization in the small intestine and colon, we aimed to further identify glial cell distribution in those layers and their response to obesity. Glial cells were detected by using S100beta (S100 calcium binding protein B) antibody in IHC analysis. In small intestinal myenteric plexus layer, S100beta is expressed in compact cell populations creating a ganglion-like shape (Figure 17A). In obese animals, even though S100beta expression doesn't change in ganglion-like structures, glial cells started to be elongated towards the submucosal layer similar to PDGFRA expression in myenteric plexus. It was shown in wild type animals that S100beta can also be observed around the crypts. Surprisingly, glial cells changed their pattern such that they were more prominent in close proximity to crypts, forming web-like structures, surrounding the crypts (Figure 17B). In colonic myenteric plexus, S100beta+ glial cells are located in smaller structures in obese animals compared to controls. Different from small intestine, those structures were observed to be elongated horizontally. On the other hand, those glial cells are also vertically elongated towards the mucosal layer, similar to small intestine myenteric plexus. Those elongated glial cells were observed to enclave the crypts in colonic epithelium (Figure 17C, D). Depending on the region of the colon, muscle layer could be observed to increase in width in obese animals (Figure 17D). Ganglia containing S100beta+ glial cells are heterogenously distributed along the myenteric plexus of both small intestine and colon, in parallel with ACOT7+ ganglia. In contrast to high fat diet, we observed no change in

the expression level or pattern of S100beta+ glial cells under Western diet conditions in both small intestine and colon compared to control (Appendix V).

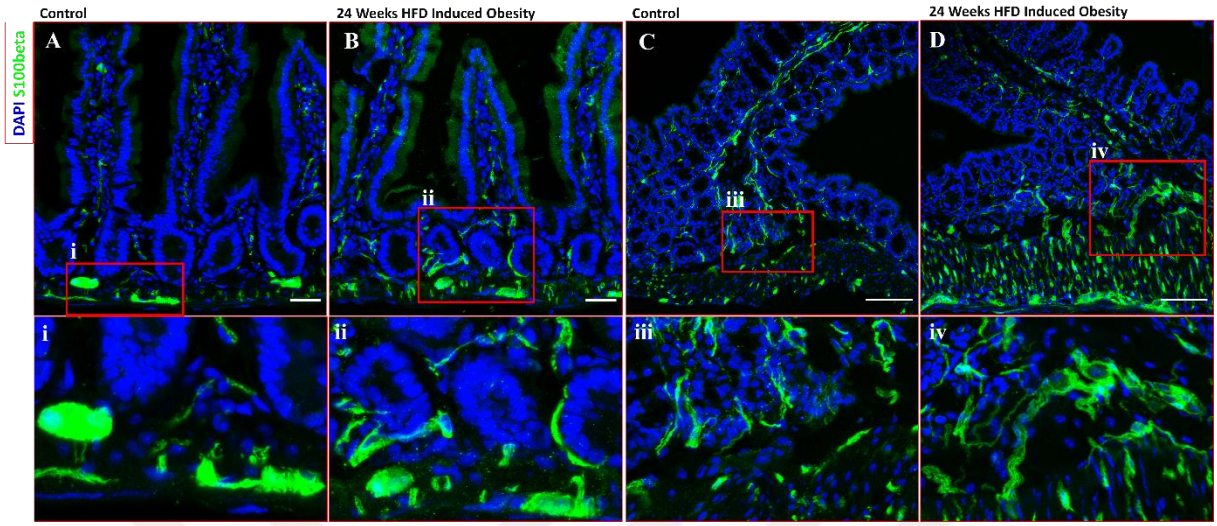

Figure 17: IHC stainings showing glial cells with S100β expression (green) in small intestine of control (A) and obese (B) animals and colon control (C) and obese (D) animals. Zoom in panels show glial cells in myenteric plexus and around the crypts of small intestine (i,ii) and colon (iii,iv).Scale bar represents 50 μm for A and B, 150 μm for C and D.

4.2.4 Interaction of Glial and Mesenchymal Cells

After detecting that glial cells constitute the main subpopulation in small intestinal and colonic extraepithelial regions affected by high fat diet induced obesity, we aimed to understand whether those glial cells function in coordination with known mesenchymal populations. To this end, we conducted series of IHC experiments with PDGFRA antibody in obesity model in tandem with S100beta. In parallel with previous observations, glial cells are increased around cryptic regions in very close proximity in obese animals (Figure 18A-B). Although PDGFRA+ cells were detected to surround the crypts in both control and obese animals, their expression levels were highly increased upon obesity (Figure 18B). Interestingly, glial cells and PDGFRA+ cells co-localized and generated a layered structure around the intestinal crypts in obese animal. In this structure, the inner layer surrounding the crypts comprised of PDGFRA+ cells while outer layer is formed by glial cells (Figure 18B). Similarly, both PDGFRA and S100beta expression were increased in myenteric plexus layer upon obesity. PDGFRA+ and glial cells were detected to be localized in the neighboring cells along the plexus layer (Figure 18A-B). Glial cells that create ganglia in the myenteric plexus were encapsulated by PDGFRA expression in both wild type and obese animals (Figure 18A-B).

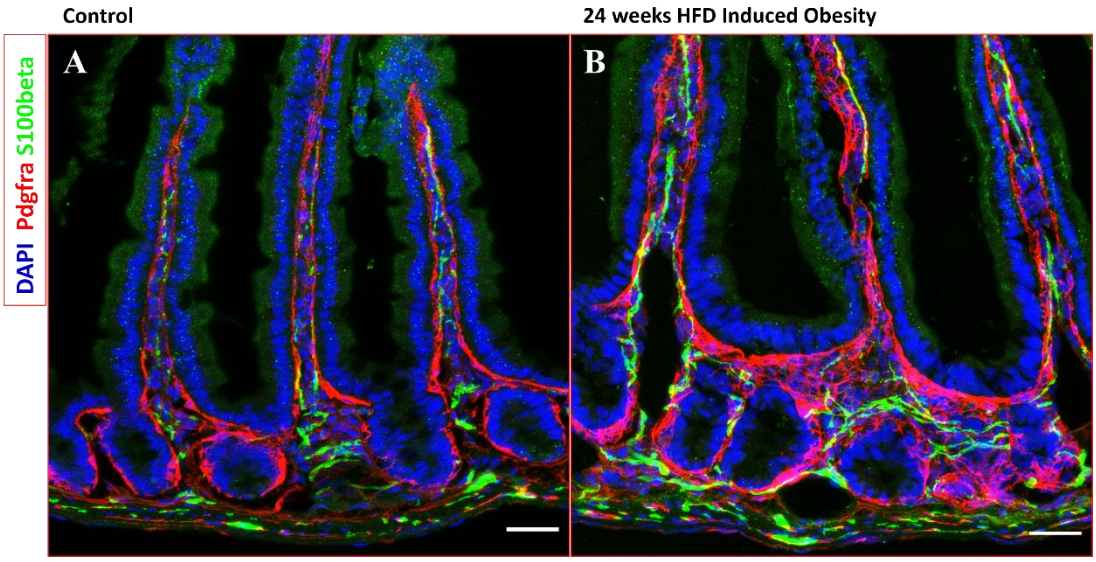

Figure 18: Small intestine IHC staining against glial cells (S100β,green) and PDGFRA+ extraepithelial cell (red). Glial cells expression was observed in both myenteric plexus layer and mesenchyme in control (A) and obese animals that were fed with high fat diet for 24 weeks (B). DAPI was used to counterstain nucleus. Scale bar represents 50 μm.

4.3 Colonic Activity Under DSS Induced Colitis Condition

DSS induced colitis is one of the widely used inflammatory disease models that distinctly affect colonic epithelium to study regeneration and activity of colonic stem cell along with its niche components. Thus, we aimed to detect the alterations of damaged and regenerated tissue in terms of neuronal and glial cells. To do so, we conducted series of IHC stainings with the markers we previously used for high fat diet induced obesity model and brain in colitis including ACOT7, HuCD, S100beta, Ki67 and PDGFRA.

4.3.1 Proliferative Cells in Colitis

After observation of proliferative cell increase upon obesity condition in small intestine and colonic epithelium, we aimed to reciprocate our results in colon in inflammation and regeneration states upon DSS administration. Also, staining of Ki67 was used to confirm damage state of colonic epithelium. During homeostasis, the proliferation rate of cycling cells is stable. In colonic epithelium, those cells are located at the bottom of the crypts (Figure 19A). In damaged tissue, stated as DSS no recovery phase, epithelium of colon was completely disrupted showing a lack of defined crypt structures even though muscle layer stays intact. This muscle layer was observed to be thickened in inflammation. We observed that, proliferative cells were decreased in number along the damaged layer (Figure 19B). When colonic tissues of model animals were induced into regeneration phase with switching DSS containing water

supply to regular drinking water, we observed newly formed crypt structures along with the remaining damaged regions. Those recently established epithelial layers were observed to contain increased number of Ki67+ cells even compared to controls. Further, remaining damaged areas show similar proliferative cell capacity with no recovery phase. Increase in the muscle layer thickness was prominent during regeneration state compared to controls (Figure 19C).

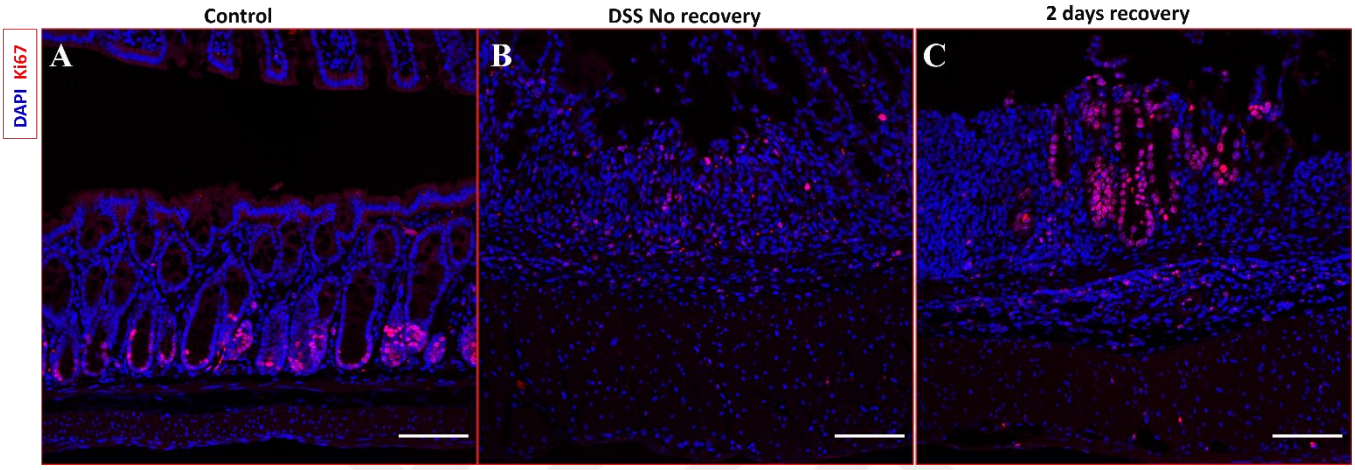

Figure 19: Proliferative cells shown by Ki67 (red) IHC stainings. Ki67+ cells can be observed at the bottom of the colonic crypts of control (A), DSS induced colitis model at inflammation state (B) and 2 days recovery phase (C) animals. Scale bar represents 150 µm.

4.3.2 Glial and Neuronal Cells in Colitis

We previously showed that ACOT7 specifically detects myenteric and submucosal ganglia cells in small intestine and colon. Also, neuron marker HuCD was observed to be colocalized with those ACOT7+ cells which were enveloped by PDGFRA+ cells. Thus, we aimed to reveal whether inflammatory disease state shows a similar cell profile specifically in colon under colitis induction. This pattern of co-expression of ACOT7 and HuCD with PDGFRA+ cells was observed in homeostasis, damaged tissue and in recovery phase of colon (Figure 20A-C). In control tissue, crypt structures were observed to be intact and organized showing prominent expression at the top of the crypts (Figure 20A). However, DSS induction caused colonic epithelium disruption showing an elevated level of PDGFRA expression along with vertical elongation of signal in myenteric plexus layer towards submucosal plexus (Figure 20B). This change in the axis of PDGFRA expression was observed in tandem with thickening of muscle layer (Figure 20B). However, we didn't detect any expression change in ACOT7 and HuCD throughout the myenteric plexus layer. Ganglionic structures (ACOT7+/HuCD+) were observed to be elongated in homeostasis state while upon injury in colon, these structures

transformed into more round shaped formations (Figure 20B). In recovery phase, we observed recently generated crypts alongside with remaining damaged tissue. Increase in PDGFRA expression at the top of the crypts and alterations of ganglia were detected to be persistent (Figure 20C).

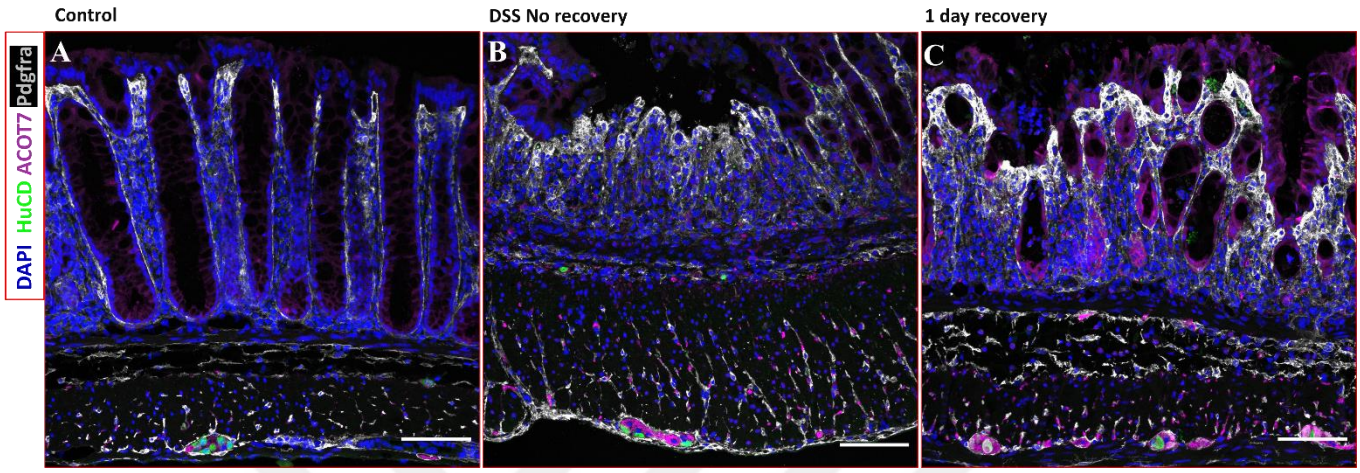

Figure 20: Colon IHC analysis showing ACOT7+ myenteric ganglia (magenta) with neurons (HuCD,green) and PDGFRA+ cells (gray) in control (A), DSS induced colitis (B) and 1 day recovery phase (C). DAPI was used to counterstain nucleus. Scale bar represents 150 µm.

We have previously described ENS composition containing neuronal and glial cells. Additionally, we detected S100beta+ glial cells as the main responders of ENS to metabolic disease condition in obesity. For this reason, we focused on colonic epithelia to check whether this response of glial cells and their interaction with PDGFRA+ cells are valid for an inflammatory disease namely colitis. S100beta+ glial cells were observed in myenteric plexus of colon similar to small intestine and those glial cells were detected to be localized in vicinity of PDGFRA+ cells in homeostasis (Figure 21A). In damaged tissue, both of those proteins were detected to be elevated in terms of their expression levels both in myenteric plexus layer and dispersed along the damaged layer. Glial cells were observed to be extended horizontally in myenteric layer in parallel with upwards localization profiles from ganglia to submucosa (Figure 21B). Regeneration phase of colon demonstrated expression level in between homeostasis and inflammation as well as joinant localization with PDGFRA+ cells (Figure 21C). When these data are taken into consideration, we could suggest an important role of glial cells and PDGFRA+ cells in response to serious injury of colonic epithelium complementary to the observation in small intestine during obesity.

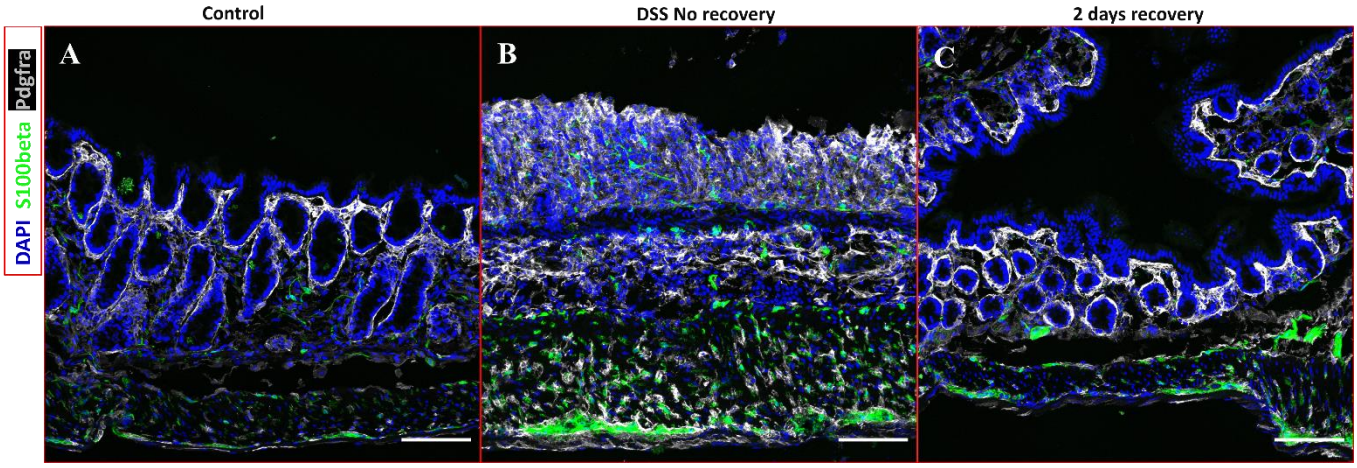

Figure 21: Colon IHC staining against glial cells (S100β,green) and PDGFRA+ extraepithelial cell (gray). Glial cells expression was observed in both myenteric plexus layer and mesenchyme in control (A), animals with damage (B) and animals in 2 days recovery phase (C). DAPI was used to counterstain nucleus. Scale bar represents 150 μm.

4.4 Gut-Brain Axis in DSS Induced Colitis

Previous studies suggest direct communication between intestine and brain in case of inflammation in the intestinal epithelium (Koren et al,2021). Thus, we aimed to explore this interaction in DSS induced colitis model in brain with several markers that we found to be crucial for intestinal functioning.

To investigate whether glial cells' and PDGFRA+ cells' interaction was affected in the brain upon gut infalmmation, we carried out series of immunohistochemical analysis of whole brain sections from DSS induced colitis model. After analyzing the whole brain regions, we decided to focus on the thalamic region specifically (Figure 22A-C). There were cell types observed to express only S100beta or only PDGFRA while co-localization of these two proteins was detected along the whole thalamus. Glial cells marked by S100beta were appeared to be the more prominent cell type in the thalamus of control brains compared to PDGFRA+ cells (Figure 22A). On the other hand, in mice with induced colitis and inflammation in their gut, we observed an increase in the PDGFRA expression in the thalamus more distinctly in the periventiruclar nuclei of thalamus (PVT) (Figure 22B). In recovery phase of the gut, we observed a lasting increase in the PDGFRA expression (Figure 22C). Those PDGFRA+ cells were observed to be appear in the shape of astrocytes alongside with the increase in expression during inflammation and regeneration. Previous studies suggest that some specific regions of the brain are responsible for the collection of peripheral inflammation cues one of which is the insular cortex (Koren et al, 2021). In light of this study, we checked for a response from

PDGFRA+ or glial cells to gut inflammation in the insular cortex and we observed analogous increment in animals with inflammation compared to controls (Appendix II).

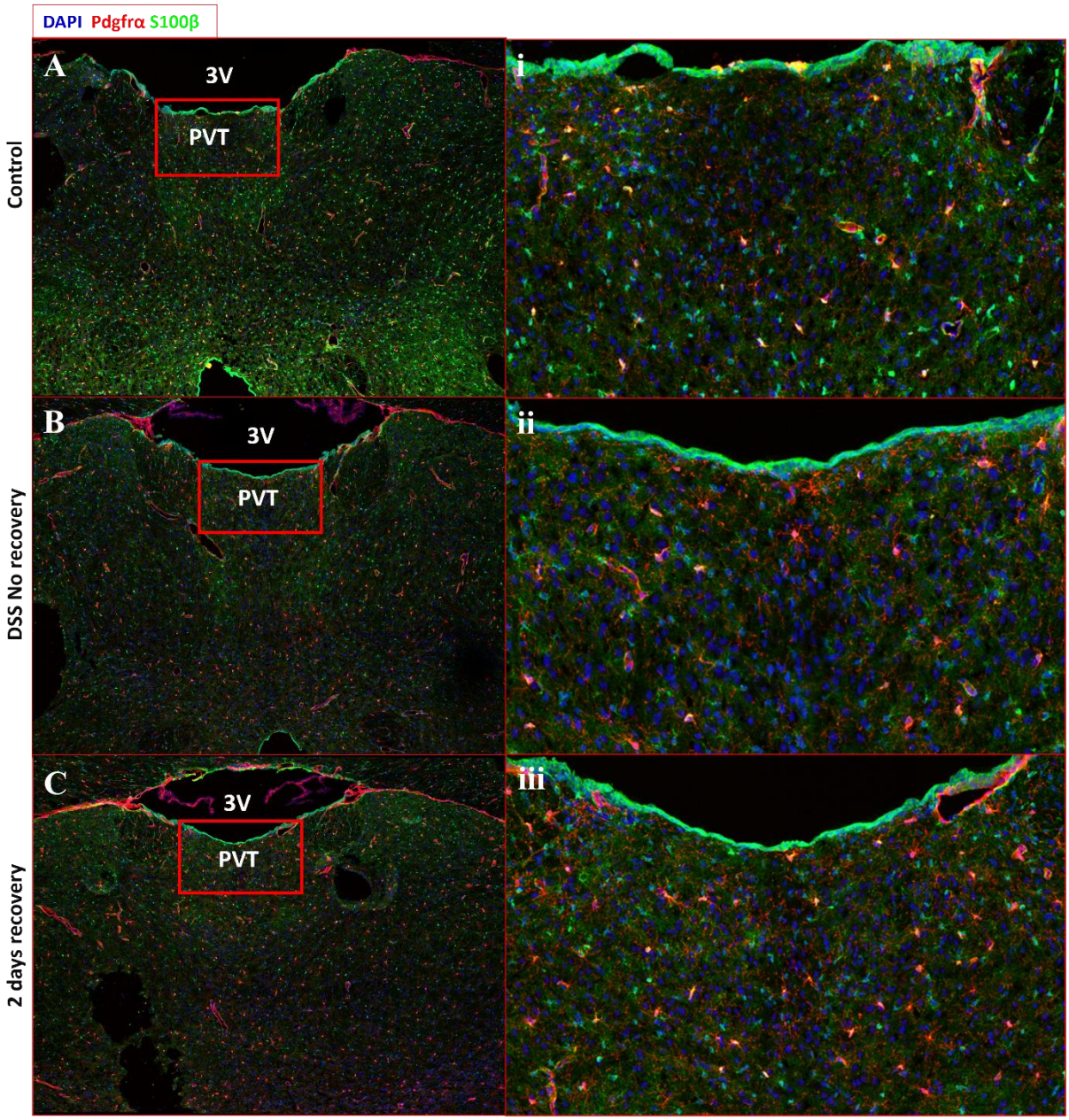

Figure 22: Tile scan images of thalamus of whole brain sections. Glial cells (S100beta, green) and PDGFRA+ cells (red) were shown by using IHC analysis on brains from animals with colitis (No recovery) and animals in recovery phase from DSS induction (2 days recovery). Thalamus is located under the 3rd ventricule (3V). Zoom in panels show expression of S100beta and PDGFRA in periventricular nucleus of thalamus (PVT) regions (i,ii,iii).

After the analysis of glial cells with S100beta expression, we aimed to observe the response of neuronal cells upon injury caused by DSS induced inflammation of gut. It was known that ACOT7 is expressed and has a crucial role in fatty acid metabolism in the brain. Surprisingly, it is highly expressed in the thalamus distributed along the region except for stria medullaris

(SM) (Figure 23A-F). On the contrary, glial cells and PDGFRA expression were observed to be located in the SM regions (Figure 22). ACOT7 was coexpressed profoundly with neurons marked by HuCD along the thalamus in all three conditions (control, inflammation, and recovery). When we focused on the PVT regions, we didn't observe any changes in the number of neurons or ACOT7+ cells upon gut injury even though there was an increase in the intensity of HuCD signal (Figure 23C,D). Similarly, HuCD+ and ACOT7+ cells didn't alter in expression or number during recovery phase (Figure 23E,F). In insular cortex, the frequency of neurons expressing HuCD was appeared to be elevated upon injury and maintained the levels during regeneration period. In addition, the coexpression of HuCD in neurons with ACOT7 was prevalent in insular cortex as well (Appendix III).

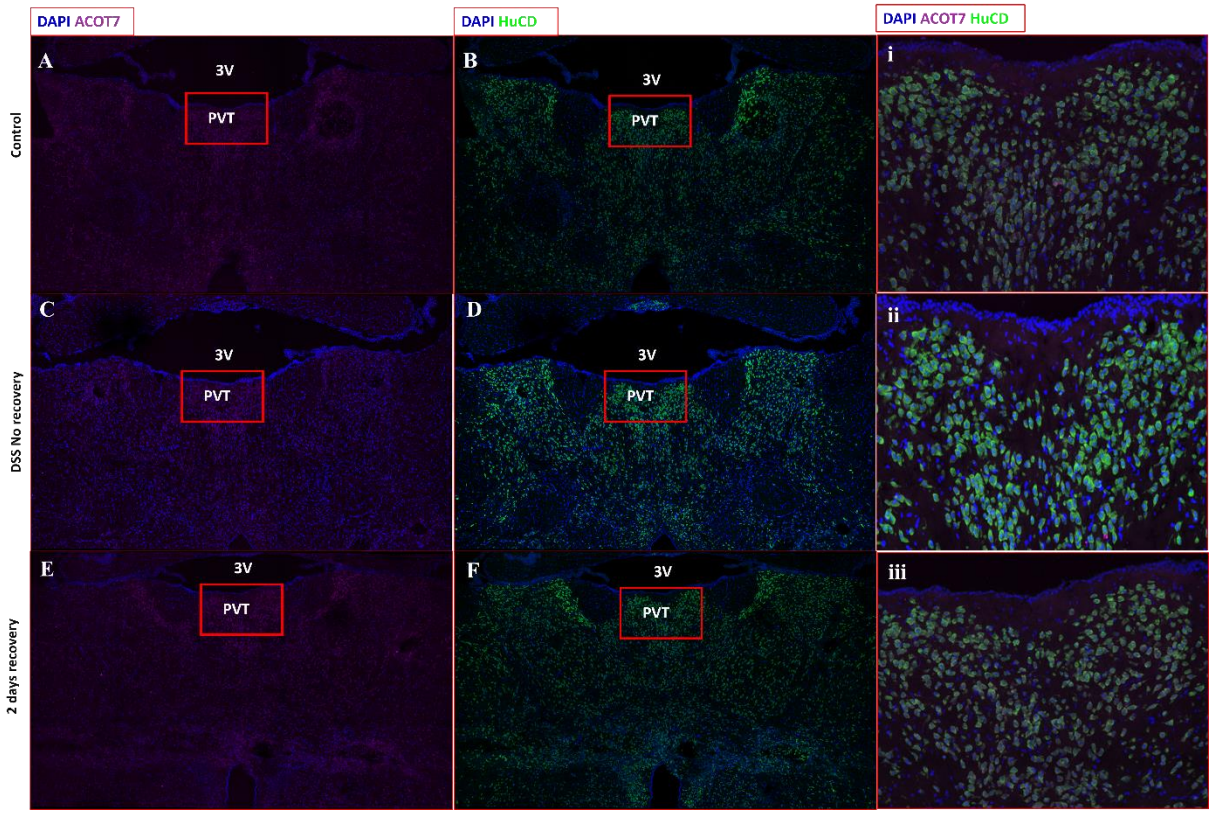

Figure 23: Tile scan images of ACOT7(magenta) and HuCD (green) IHC stainings of whole thalamus regions from control (A,B), DSS induced colitis (C,D) and recovery (E,F) animals. Zoom in panels show overlapping expressions of ACOT7 and HuCD in periventricular nucleus of thalamus (PVT) regions (i,ii,iii,). (3V: 3rd ventricule)

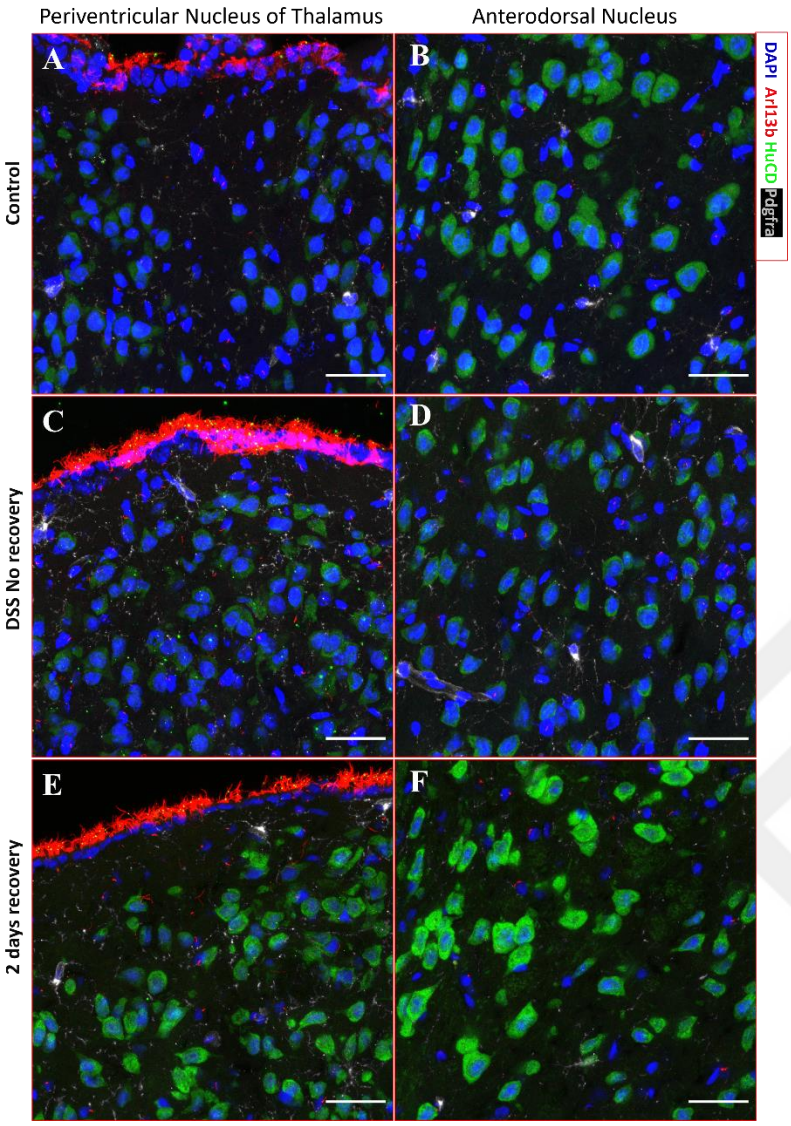

Figure 24: Primary cilia were detected dispersely along the thalamus by using IHC staining with Arl13b(red). To be able to detect ciliated cell subpopulations, neuron marker HuCD (green) and PDGFRA (gray) were used. Their colocalization can be observed in PVT and AD regions of control (A,B), no recovery (C,D) and 2 days recovery (E,F). Scale bar represents 50µm. (PVT: Periventricular nucleus of thalamus, AD: Anterodorsal nucleus).

4.4.1 Ciliated Cell Response to Colitis in Brain

It was known from previous studies that ciliated cells in subpopulations of neuronal and glial cells however their response upon gut inflammation has remained unclear. By using IHC analysis of primary cilia and neurons under colitis conditions, we observed ciliated cell populations along the whole brain. Subventicular ependymal cells were described to be ciliated which we observed same expression pattern in these series of experiments as well (Figure 24A,C,E). The majority of primary cilia weren't expressed neither by HuCD+ neurons nor by PDGFRA+ cells. However, a few number of HuCD+ neurons were observed to be ciliated while they didn't co-express PDGFRA. In PVT zone, there was a slight increase in the number of primary cilia upon injury which lasted during regeneration period. When we focused on HuCD+ neurons, we did not detect any discernible change in expression or number (Figure 24A,C,E). On the other hand, anterodorsal nucleus didn't appear to change its ciliated cell population

whereas HuCD+ neuron cell bodies were observed to be decreased in size upon injury. This shrinkage was detected to be recovered during regeneration (Figure 24B, D, F). However, since neuron size alterations are decided in a multifactorial process, this observation remains unconclusive and should be validated with further analyses.

5. DISCUSSION

In this thesis, we aimed to identify the response of small intestinal and colonic cell subpopulations upon metabolic and inflammatory disease conditions. As previously described in several studies, alterations in dietary habits have an immense impact on intestinal stem cell activity and defined structure. Similar cases were observed when colonic epithelium is disrupted by using DSS induction causing an inflammatory state. Thus, to be able to mimic metabolic disease state, we developed high fat diet induced obesity model in which experimental mice were fed with 60% fat containing diet for 24 weeks. At the end of this period, experimental groups reached thrice of their normal weight considered as obese. Initially, we confirmed that proliferation rate of crypt base cells in small intestine and colon was increased in obese animals. In terms of structural effects, small intestine didn't display any discernible damage in their villus and crypt structures whereas colonic crypts were shortening. This decrease in crypt size despite the expansion in the proliferative cells could be resulted from a change in the differentiation rate or decreased turnover capacity. However, this speculation needs to be further characterized with functional assays. Apart from proliferative cell activity, we aimed to detect specific epithelial and extraepithelial cell behaviors in obesity disease. To this end, we carried out IHC experiments with CD34 for mesenchymal niche, Lysozyme for Paneth cell which is main epithelial niche and Muc2 to mark Goblet cells. CD34+ cells were defined to be a crucial mesenchymal niche population for intestinal stem cell activity (Stzepourginski et al, 2017). In obese animals, CD34 expression were diminished in the pericryptical zone of both colon and small intestine upon obesity. This could be resulted from decreased dependency of intestinal stem cells to their niche components as previously shown (Beyaz et al,2016). As opposed to their findings, we observed no change in Paneth cell number upon high fat diet, however, this observation requires further supportive analyses. Goblet cells are the prominently found cell population dispersed in intestinal epithelium especially in colon. It is responsible for mucus secretion involved in barrier generation against bacterial communities. In obese animals, we didn't observe any change in the expression of Muc2 in small intestine as opposed to colon in which its expression was noticeably decreased. This decrease in the mucin secretion could resulted in an interruption of barrier function specifically in colon. Additionally, we observed lysozyme expression in several Goblet cells and Muc2 expression in some of the enterocytes rather than Goblet cells in obese animals. This alteration in the patterning of markers could be stemmed from misdifferentiation of secretory lineage. Higher fatty acid composition of long-term diet regimen could drive stem cell differentiation in

a diverted manner to be able to adjust environmental cues. To confirm the elevation in stem cell activity, we used several stem cell markers including Olfm4 which is vigorously expressed in CBC cells and Sox9. However, our data didn't reveal a surge in both Olfm4 and Sox9 in small intestinal epithelium. The reason behind these contrasting results could be that Lgr5 is the main stem cell marker of intestine which is used in the previous studies. Its expression pattern could be divergent from Olfm4 and Sox9. Interestingly, Sox9 was observed to be expressed in the myenteric plexus ganglia which shows that Wnt signaling could be utilized in neuronal or glial cells of intestine. The striking point of this line of experiments is that we identified primary cilia bearing cells in the intestinal extraepithelial layers including mesenchyme in close proximity to crypts, submucosal and myenteric plexuses. It was detected by using Arl13b protein and PCNT to observe full structure. Hedgehog signaling is a very essential component to coordinate intestinal architecture while primary cilia is involved in the Hedgehog signal transduction, those ciliated cell populations could be described as stem cell niche components. To be able to understand the role of those ciliated cells in disease state, we conducted IHC experiments in obese animals. However, number of primary cilia remained unchanged. Primary cilia were observed to be highly heterogeneously distributed along the tissue such that they didn't strictly confine to any specific regions. The turnover rate of cilia could also have an effect on this observation.

Novelty of this study branches from the detection of a global marker for enteric nervous system, namely ACOT7. Enteric nervous system is composed of myenteric and submucosal ganglia which ACOT7 marks both. To characterize its distinct cell types, we used E-cadherin and commonly used mesenchymal marker PDGFRA for IHC analysis. ACOT7 was found to be expressed by ganglia cells and specifically Tuft cells in the epithelium. Also, PDGFRA+ cells were observed to envelop those myenteric ganglia explicitly defining borders of ACOT7+ cells. Similar to primary cilia, ACOT7+ ganglia were heterogeneously distributed along the intestinal tissue not having a definite pattern. Further, staining with αSMA confirmed that ACOT7+ cells compose the enteric nervous system cells but not muscle or fibroblast cells. These ACOT7+ cells were observed to be embedded in the muscle layer and their localization distributed along muscles didn't change upon high fat diet induced obesity. We previously detected the presence of ciliated cells along the myenteric and submucosal layers of small intestine and colon. Those ciliated cells were detected to co-express ACOT7 protein in those layers however, not all subtypes of cells in the ganglia contain primary cilia. This differential expression of Arl13b could be caused by the diverse functions of heterogenous cell populations since we believe that

not all complex ganglia structures marked by ACOT7+ carry the same role along the myenteric plexus.

Enteric nervous system has a crucial role to relay environmental signals to the central nervous system and their signaling center could be the intermingled network of neurons and glial cell populations namely ganglia. After defining ACOT7 distinctly specify those ganglia as a whole complex, we aimed to characterize the composition of those structures in intestine. Thus, HuCD, a highly studied neuron body marker and PHOX2B to detect neuron nucleus were selected for histology analysis. Both markers were observed to be co-expressed in ACOT7+ cells in myenteric and submucosal plexuses specifically in the expanded region of the ganglia. Thus, we can conclude that those main bodies are composed prominently of neurons. However, elongated pattern of ACOT7 expression were detected not to be comprised of neuron bodies marked by HuCD or PHOX2B. Hence, ACOT7+ ganglionic cells are not solely neuronal but rather they could be mixture of neurons and glial cells. To confirm that, we could use S100beta which marks particularly all types of glial cells but not a specific sub-population such as astrocytes or microglia for further characterization. After that, we can fully understand the composition of those ACOT7+ cells in the myenteric ganglia. If those extensions of ACOT7 are detected to be glial cells, we can describe ACOT7 as a global marker for enteric nervous system network in small intestine and colon. Additionally, we used Tuj1 as neurofilament marker in the same setup and we observed expression in myenteric plexus layer, submucosal plexus, and lamina propria of the small intestine. We didn't observe change neuron filaments in the obese animals. In obesity condition, it was known that stem cells and niche components differentially react to the increased fatty acid levels in the intestinal microenvironment nonetheless involvement of enteric nervous system cells have not been studied yet. When we checked for neuron response with HuCD and PHOX2B along with the ACOT7 expression, we observed no visible changes in obese animals' intestine neither in expression nor in composition in ganglia. Thus, we can conclude that neurons were not the main driver for the relay of metabolic cues. We previously observed that Sox9 is expressed in the myenteric plexus layer which can be suggested as Wnt/beta catenin signaling. In parallel, Beta catenin expression was detected in the myenteric ganglia completely overlapping the ACOT7 expression. Thus, we can strongly speculate the prevalence of Wnt/Beta catenin pathway in the cells of enteric nervous system. Also, we didn't detect any changes of expression pattern or localization of beta catenin signal upon obesity. To be able to characterize primary cilia possessive cells in the myenteric plexus, we used HuCD neuron marker alongside with Arl13b. Both colonic and small intestinal

ganglia showed heterogenous co-expression of primary cilia in neurons. Ganglionic structures were defined with Pdgfra+ cells and inside these networks HuCD+ and HuCD- cells were distinguished. Further characterization revealed that those cells were subdivided into Arl13b+ and Arl13b- clusters. When PDGFRA expression was assessed in this experimental setup, it was revealed that horizontally expressed PDGFRA pattern in controls was diverted to a vertical manner towards the submucosal plexus layer in obese animals notably in colon. This diversion could be explained either by migration of PDGFRA+ cells towards the submucosal layer generating a bridge between ENS and epithelium or by rotation of Pdgfra+ cells to a vertical position such that a similar network is constructed.

Since we didn't detect any response by ACOT7+ ganglionic cells towards high fat diet regimen, next step was to analyze glial cells in the myenteric plexus layer. Interestingly, S100beta expression was observed in myenteric ganglia, submucosal plexus and pericryptical regions of both small intestine and colon. Upon obesity, S100beta expression was not only increased in myenteric plexus layer and pericryptical zone but also branched out around the intestinal and colonic crypts. Similar to PDGFRA+ cells, glial cells were detected to be emanated in an upwards motion from myenteric ganglia towards submucosal layer particularly in colonic muscle layer. This shift in expression pattern wasn't that evident in small intestine could be caused by the relatively narrow muscle layer when compared to colon. Since comparable expression levels of ACOT7 and HuCD in control and obese animals were observed, along with the fact that glial cells are immensely increased in obese animals, we may strongly suggest glial cells to be the core activated cell population responding to metabolic changes in ENS rather than neurons. Glial cells are defined to have diverse functions and supportive roles than neurons, we could speculate that they could have acquired a more adaptive role in ENS. Due to the fact that environmental signals in obesity condition are changed depending on the long-term diet, S100beta+ glial cells were speculated to participate in the collection and relay of such cues. Additionally, glial cells are described to have extended migration capabilities. Since we couldn't detect whether S100beta+ cells migrated from myenteric plexus towards the pericrytptical regions or resident glial cells upregulated their S100beta expression upon obesity, further characterization would be required to reveal the reason behind this response of glial cells. In small intestine, we checked whether those activated glial cells are interacting with resident niche populations. Thus, we used prominent mesenchymal marker PDGFRA along with S100beta because we observed similar changes in the expression patterns of those proteins in obese animals. Also, a previous study has described the crucial role of enteric glial cells in

case of infection and inflammation to provide tissue repair in coordination with immune cells via cytokines (Progatzky et al, 2021). Even though this finding supports our hypothesis on glial cell function in metabolic diseases, we additionally described a stratified layer formation with PDGFRA+ mesenchymal cells and glial cells around the crypts of small intestine. This layered structure demonstrated that PDGFRA+ cells could create a bridge between intestinal stem cells and glial cells. Since those mesenchymal cells are located closer to the epithelium, it could be reasonable to speculate that there couldn't be any direct interactions between glial cells and stem cells. Also, increase in PDGFRA expression in parallel with S100beta expression in disease state supports our hypothesis on their coordinated function and localization around the crypts.

High regeneration capacity of intestinal crypts arises from the actively proliferating cell pools. In order to detect response of those proliferating cells in case of an epithelial damage, we conducted IHC experiments on DSS induced damage in colonic crypts. The proliferation rate is balanced to preserve distinct structure of colonic epithelia provided by proliferative cells located at the bottom of crypts during homeostasis. However, when this epithelial layer is disrupted, those cells were also damaged such that Ki67 expression was observed to be decreased in colitis model compared to control. In recovery phase, we can distinguish the newly generated crypts with higher proliferative capacity to reestablish damaged structure to a healthy state. Recovering tissue also showed remaining damaged layers which have diminished Ki67 expression similar to injured tissue. With these data, we confirmed the high regenerative capacity of colonic crypts upon injury. High fat diet induced obesity as a dietary model provide us with great insights into the composition of ENS subpopulations and response of ENS towards environmental changes. Conclusively, S100beta+ glial cells were detected to be elevated in higher levels of fatty acids in both colon and small intestine. To further understand the role and change of ENS subclusters including ACOT7+ ganglia, HuCD+ neurons, S100beta+ glia and PDGFRA+ extraepithelial cells, we generated DSS induced colitis model mimicking colon inflammation. We observed that ACOT7 was co-expressed with HuCD and ACOT7+ myenteric ganglia were encapsulated with PDGFRA expression in homeostasis, damaged and recovering tissue. Even though the ACOT7 expression level didn't change tissue-wise, ganglia expressing ACOT7 were altered in their shape becoming rounder structures. This effect was speculated to be resulted from the constriction of muscle layer in colon upon inflammation such that elongated cell populations were pulled towards each other upon shortening of the colon. Additionally, PDGFRA expression was observed to be evidently increased in damaged

epithelium alongside with the change in the rotation of PDGFRA signal in myenteric plexus. This data was overlapping the observations in small intestine of obese animals. Change in the pattern of PDGFRA expression could be an indicator of PDGFRA+ cells in signal transduction between mesenchymal layers and myenteric ganglia. In parallel with obesity model, we observed that S100beta+ glial cells were increased in both injured and recovering colon. Those cells were detected to be localized alongside with PDGFRA+ cells in both myenteric plexus and disrupted epithelial layer. High fat diet obesity and DSS induced colitis models consistently provide us with greater understanding on damage response of ENS in cooperation with extraepithelial cells in small intestine and colon. Even though high fat diet didn't cause as severe damage as DSS induction did, any shift in the homeostasis of microenvironment triggers ENS to activate specific cell populations and forces a structural or localization adjustment.

Gut-brain axis has been considered as a hot topic in recent years after identification of the importance of ENS in homeostatic functioning of intestines. After analyzing a recently published study, we sought to investigate the response of brain regions to DSS induced colitis to observe whether similar activation patterns were prominent in CNS, specifically in brain. Thus, initially we focused on ACOT7 expression along with the HuCD+ neurons in whole brain sections. After careful considerations, we decided to focus on the thalamic regions and insular cortex due to the previous studies showing their involvement in collection of inflammatory information from the gut (Koren et al, 2021). Our IHC analysis revealed that ACOT7 is highly co-expressed along the whole thalamus with HuCD which we can conclude that ACOT7 predominantly marks neurons in brain different from ENS. Nevertheless, we didn't detect any changes in the expression levels of neither HuCD nor ACOT7 in the thalamus. Interestingly, PDGFRA was expressed in both thalamus and insular cortex in a dispersed manner along with the glial cells. When we checked their localization in thalamus, we detected that S100beta+ glial cells were primarily localized in thalamus rather than PDGFRA+ cells in wild type animals whereas brain sections with inflammation upon DSS treatment revealed a reversed localization pattern. This effect was retained during recovery phase of gut after inflammation. Also, we observed several glial cells that co-express PDGFRA. This increase in PDGFRA expression was mainly detected in periventricular nucleus of thalamus (PVT). Also, upon DSS treatment, S100beta expression was appeared to be diminished however we couldn't conclude whether it is resulted from elevated co-localization with PDGFRA or rather from an actual reduction in protein level. Aside from glial cells, PDGFRA+ cells were observed to transform into astrocyte-like shaped structures during inflammation and regeneration phase of the colon. A recent study

defining PDGFRA+ cell type inside the lateral ventricles suggested that those cell type can be described as intraventricular oligodendrocyte progenitors and their function is to relay signals from cerebrospinal fluid and communication with other neuron axons (Delgado et al, 2021). Additionally, glial and neuronal cell types were produced from astrocyte-shaped neuronal stem cells located in subventricular zone of the brain (Doetsch et al, 1999). Another study described the PDGFRA+ cell population in this zone as neuronal stem cells giving rise to oligodendrocytes as well. However, elimination of those PDGFRA+ cells in subventricular zone disrupts oligodendrocyte generation rather than neurons (Jackson et al, 2006). In light with those findings, we could hypothesize that injury in the gut induced by DSS treatment causes an elevation of PDGFRA+ cells that behold stem cell properties in thalamic regions which should be further examined with functional analysis. A hallmark study showed that those PDGFRA+ astrocytic stem cells in the boundary of ventricles possess a single cilium whereas lower layer of ependymal cells can contain multiple number of cilia (Doetsch et al, 1999) In our study, we demonstrated those multiply ciliated cell populations around 3rd ventricle in PVT region with Arl13b expression confirming the previous observation. Also, we observed a slight increase in the number of ciliated cells in PVT region in inflammation state of colon while anterodorsal nucleus area didn't yield any changes in terms of cilia number. Those ciliated cells were detected to be heterogeneously expressed in HuCD+ neurons and HuCD- subpopulations along the thalamus. In terms of HuCD expression, we observed a decrease in cytoplasm density of neurons in the brains of DSS induced colitis model animals. However, we couldn't decisively claim that this is indeed caused by a disease state such that there are multiple factors affecting neuron size.

6. CONCLUSION AND FUTURE PERSPECTIVES

In this study, we found that primary cilia are produced in small intestinal mesenchymal cells. We identified a cell population in the myenteric plexus and submucosal plexus of intestine that is specifically marked by ACOT7 enzyme. This enzyme was found to explicitly identify enteric nervous system elements including glial and neuronal cells. Also, in these populations, we showed that ACOT7 was colocalized with primary cilia under colitis and obesity conditions along with the homeostatic state. We hypothesized that enteric nervous system has a connection with stem cell niche under metabolic conditions. Thus, we aimed to classify ACOT7+ and primary cilia positive cell subpopulations and reveal their response upon DSS and high fat diet application. In order to assess our hypotheses, we conducted series of IHC experiments with known glial and neuronal markers in mice colitis and obesity models. We showed that S100beta+ cells are the main populations in ENS that respond to changes in intestine upon high fat diet administration. Similar results were acquired upon DSS induction specifically in colon. Further, we observed that S100beta+ cells are colocalized with PDGFRA+ mesenchymal cells that are in close proximity to crypt base columnar stem cells in both homeostasis and disease. Also, we observed a prominent elevation of both PDGFRA and S100beta expression in those disease models. However, the interaction mechanism remains unclear. After detecting this interaction in intestine upon colitis, we further aimed to reveal whether the same effect is exerted in the brain, specifically in thalamus. Expectedly, we observed similar increase in expression of PDGFRA in injury state aside from its co-expression with S100beta+ glial cells. These results suggest the importance of communication through gut-brain axis.

Our current goal is to identify this interaction mechanism between mesenchymal and glial cells in intestine with several *ex vivo* setups including co-cultures of intestinal organoids with both glial and mesenchymal cell populations. Additional functional analysis including elimination of either PDGFRA+ or glial cells to observe intestinal reaction towards disease conditions. Moreover, paired sequencing could be a fruitful tool to detect the signals involved in communication of these tightly colocalized cells along with the common pathways they are contributing to. Since ACOT7 has been described as a novel ENS marker, knock out studies of this protein could be carried out to unravel the specific role of ACOT7 in intestinal homeostasis and regeneration.

Overall, our novel finding is that ACOT7 can be used a marker for both submucosal and myenteric plexus of enteric nervous system. Additionally, we suggest that extraepithelial niche components and enteric nervous system respond to both higher fat composition in the diet

mimicking obesity conditions and to ulcerative colitis by DSS induction. Ciliated cells are concomitant in subpopulations of both mesenchymal cells and ENS components.

REFERENCES

Agustí, A., García-Pardo, M. P., López-Almela, I., Campillo, I., Maes, M., Romaní-Pérez, M., & Sanz, Y. (2018). Interplay between the gut-brain axis, obesity and cognitive function. *Frontiers in neuroscience,* 12, 155.

Aoki, R., Shoshkes-Carmel, M., Gao, N., Shin, S., May, C. L., Golson, M. L., ... & Kaestner, K. H. (2016). Foxl1-expressing mesenchymal cells constitute the intestinal stem cell niche. *Cellular and molecular gastroenterology and hepatology*, *2*(2), 175-188.

Baghdadi, M. B., Ayyaz, A., Coquenlorge, S., Chu, B., Kumar, S., Streutker, C., ... & Kim, T. H. (2021). Enteric glial cell heterogeneity regulates intestinal stem cell niches. *Cell stem cell.*

Bangs, F., & Anderson, K. V. (2017). Primary cilia and mammalian hedgehog signaling. *Cold Spring Harbor perspectives in biology*, *9*(5), a028175.

Barker, N., Van Es, J. H., Kuipers, J., Kujala, P., Van Den Born, M., Cozijnsen, M., ... & Clevers, H. (2007). Identification of stem cells in small intestine and colon by marker gene Lgr5. *Nature*, *449*(7165), 1003-1007.

Barker, N. (2014). Adult intestinal stem cells: critical drivers of epithelial homeostasis and regeneration. *Nature reviews Molecular cell biology*, *15*(1), 19-33.

Bergeron, S., Lemieux, E., Durand, V., Cagnol, S., Carrier, J. C., Lussier, J. G., ... & Rivard, N. (2010). The serine protease inhibitor serpinE2 is a novel target of ERK signaling involved in human colorectal tumorigenesis. *Molecular cancer*, *9*(1), 271.

Beyaz, S., Mana, M. D., Roper, J., Kedrin, D., Saadatpour, A., Hong, S. J., ... & Pinello, L. (2016). High-fat diet enhances stemness and tumorigenicity of intestinal progenitors. *Nature*, *531*(7592), 53-58.

Büller, N. V., Rosekrans, S. L., Westerlund, J., & van den Brink, G. R. (2012). Hedgehog signaling and maintenance of homeostasis in the intestinal epithelium. *Physiology*, *27*(3), 148-155.

Cenit, M. C., Sanz, Y., & Codoñer-Franch, P. (2017). Influence of gut microbiota on neuropsychiatric disorders. *World journal of gastroenterology*, 23(30), 5486.

Chan, A. T., & Giovannucci, E. L. (2010). Primary prevention of colorectal cancer. *Gastroenterology*, *138*(6), 2029-2043.

Clevers, H. C., & Bevins, C. L. (2013). Paneth cells: maestros of the small intestinal crypts. *Annual review of physiology*, *75*, 289-311.

Cryan, J. F., O'Riordan, K. J., Cowan, C. S., Sandhu, K. V., Bastiaanssen, T. F., Boehme, M., ... & Dinan, T. G. (2019). The microbiota-gut-brain axis. *Physiological reviews*.

Degirmenci, B., Valenta, T., Dimitrieva, S., Hausmann, G., & Basler, K. (2018). GLI1-expressing mesenchymal cells form the essential Wnt-secreting niche for colon stem cells. *Nature*, *558*(7710), 449-453.

Delgado, A. C., Maldonado-Soto, A. R., Silva-Vargas, V., Mizrak, D., von Känel, T., Tan, K. R., ... & Doetsch, F. (2021). Release of stem cells from quiescence reveals gliogenic domains in the adult mouse brain. *Science*, *372*(6547), 1205-1209.

Delling, M., DeCaen, P. G., Doerner, J. F., Febvay, S., & Clapham, D. E. (2013). Primary cilia are specialized calcium signalling organelles. *Nature*, *504*(7479), 311-314.

Doetsch, F., Caille, I., Lim, D. A., García-Verdugo, J. M., & Alvarez-Buylla, A. (1999). Subventricular zone astrocytes are neural stem cells in the adult mammalian brain. *Cell*, *97*(6), 703-716.

Doetsch, F., García-Verdugo, J. M., & Alvarez-Buylla, A. (1999). Regeneration of a germinal layer in the adult mammalian brain. *Proceedings of the National Academy of Sciences*, *96*(20), 11619-11624.

Drokhlyansky, E., Smillie, C. S., Van Wittenberghe, N., Ericsson, M., Griffin, G. K., Eraslan, G., ... & Regev, A. (2020). The human and mouse enteric nervous system at single-cell resolution. *Cell*, 182(6), 1606-1622.

Ellis, J. M., Wong, G. W., & Wolfgang, M. J. (2013). Acyl coenzyme A thioesterase 7 regulates neuronal fatty acid metabolism to prevent neurotoxicity. *Molecular and cellular biology*, 33(9), 1869-1882.

Ellis, J. M., Bowman, C. E., & Wolfgang, M. J. (2015). Metabolic and tissue-specific regulation of acyl-CoA metabolism. *PloS one*, 10(3), e0116587.

Farin, H. F., Van Es, J. H., & Clevers, H. (2012). Redundant sources of Wnt regulate intestinal stem cells and promote formation of Paneth cells. *Gastroenterology*, *143*(6), 1518-1529.

Fodde, R., Schmitt, M., Schewe, M., & Augenlicht, L. H. (2017). Modelling western dietary habits in the mouse: easier said than done. *Hepatobiliary surgery and nutrition*, *6*(2), 138.

Furness, J. B. (2012). The enteric nervous system and neurogastroenterology. Nature reviews *Gastroenterology & hepatology*, 9(5), 286-294.

Gabella, G. (1981). Ultrastructure of the nerve plexuses of the mammalian intestine: the enteric glial cells. *Neuroscience*, 6(3), 425-436.

Gershon, M. D. (1997). Genes and lineages in the formation of the enteric nervous system. *Current opinion in neurobiology*, 7(1), 101-109.

Gulbransen, B. D., & Sharkey, K. A. (2012). Novel functional roles for enteric glia in the gastrointestinal tract. *Nature reviews Gastroenterology & hepatology*, 9(11), 625-632.

Graham, K. D., López, S. H., Sengupta, R., Shenoy, A., Schneider, S., Wright, C. M., ... & Heuckeroth, R. O. (2020). Robust, 3-dimensional visualization of human colon enteric nervous system without tissue sectioning. *Gastroenterology*, 158(8), 2221-2235.

Hilgendorf, K. I., Johnson, C. T., Mezger, A., Rice, S. L., Norris, A. M., Demeter, J., ... & Jackson, P. K. (2019). Omega-3 fatty acids activate ciliary FFAR4 to control adipogenesis. *Cell*, *179*(6), 1289-1305.

Iruzubieta, P., Cantarero, I., Monzón, M., Lahoz, M., & Junquera, C. (2020). Supporting Evidence of Human Enteric Nervous System Adult Neurogenesis: Presence of Primary Cilia and Adult Neurogenesis Markers. *Cellular and Molecular Neurobiology*, 1-9.

Jackson, E. L., Garcia-Verdugo, J. M., Gil-Perotin, S., Roy, M., Quinones-Hinojosa, A., VandenBerg, S., & Alvarez-Buylla, A. (2006). PDGFRA-positive B cells are neural stem cells in the adult SVZ that form glioma-like growths in response to increased PDGF signaling. *Neuron*, *51*(2), 187-199.

Junquera Escribano, C., Cantarero Carmona, I., Luesma Bartolomé, M. J., Soriano Navarro, M., Martínez Ciriano, C., Castiella Muruzabal, T., & García-Verdugo, J. M. (2011). The primary cilium: a relevant characteristic in interstitial cells of rat duodenum enteric plexus. *Histology and histopathology*, Vol. 26, nº 4 (2011).

Kang, H. W., Niepel, M. W., Han, S., Kawano, Y., & Cohen, D. E. (2012). Thioesterase superfamily member 2/acyl-CoA thioesterase 13 (Them2/Acot13) regulates hepatic lipid and glucose metabolism. *The FASEB Journal*, 26(5), 2209-2221.

Katoh, Y., & Katoh, M. (2006). Hedgehog signaling pathway and gastrointestinal stem cell signaling network. *International journal of molecular medicine*, *18*(6), 1019-1023.

Kinchen, J., Chen, H. H., Parikh, K., Antanaviciute, A., Jagielowicz, M., Fawkner-Corbett, D., ... & Simmons, A. (2018). Structural remodeling of the human colonic mesenchyme in inflammatory bowel disease. *Cell*, *175*(2), 372-386.

Kong, S., Zhang, Y. H., & Zhang, W. (2018). Regulation of intestinal epithelial cells properties and functions by amino acids. *BioMed research international*, *2018*.

Koren, T., Amer, M., Krot, M., Boshnak, N., Ben-Shaanan, T. L., Azulay-Debby, H., ... & Rolls, A. (2021). Insular cortex neurons encode and retrieve specific immune responses. *Cell*.

Kuhnert, F., Davis, C. R., Wang, H. T., Chu, P., Lee, M., Yuan, J., ... & Kuo, C. J. (2004). Essential requirement for Wnt signaling in proliferation of adult small intestine and colon revealed by adenoviral expression of Dickkopf-1. *Proceedings of the National Academy of Sciences*, *101*(1), 266-271.

Kuramochi, Y., Takagi-Sakuma, M., Kitahara, M., Emori, R., Asaba, Y., Sakaguchi, R., ... & Yamada, J. (2002). Characterization of mouse homolog of brain acyl-CoA hydrolase: molecular cloning and neuronal localization. *Molecular brain research*, 98(1-2), 81-92.

Li, W., Zimmerman, S. E., Peregrina, K., Houston, M., Mayoral, J., Zhang, J., ... & Augenlicht, L. H. (2019). The nutritional environment determines which and how intestinal stem cells contribute to homeostasis and tumorigenesis. *Carcinogenesis*, *40*(8), 937-946.

Liao, W. C., Liao, C. K., Tsai, Y. H., Tseng, T. J., Chuang, L. C., Lan, C. T., ... & Liu, C. H. (2018). DSE promotes aggressive glioma cell phenotypes by enhancing HB-EGF/ErbB signaling. *PLoS One*, *13*(6), e0198364.

Malicki, J. J., & Johnson, C. A. (2017). The cilium: cellular antenna and central processing unit. *Trends in Cell Biology*, *27*(2), 126-140.

McCarthy, N., Manieri, E., Storm, E. E., Saadatpour, A., Luoma, A. M., Kapoor, V. N., ... & Wucherpfennig, K. (2020). Distinct mesenchymal cell populations generate the essential intestinal BMP signaling gradient. *Cell Stem Cell*, *26*(3), 391-402.

McMahon, A. P., Joyner, A. L., Bradley, A., & McMahon, J. A. (1992). The midbrain-hindbrain phenotype of Wnt-1− Wnt-1− mice results from stepwise deletion of engrailed-expressing cells by 9.5 days postcoitum. *Cell*, 69(4), 581-595.

Morarach, K., Mikhailova, A., Knoflach, V., Memic, F., Kumar, R., Li, W., ... & Marklund, U. (2021). Diversification of molecularly defined myenteric neuron classes revealed by single-cell RNA sequencing. *Nature neuroscience*, 24(1), 34-46.

Newmark, H. L., Lipkin, M., & Maheshwari, N. (1990). Colonic hyperplasia and hyperproliferation induced by a nutritional stress diet with four components of Western-style diet. *JNCI: Journal of the National Cancer Institute*, *82*(6), 491-496.

Nusse, R., & Clevers, H. (2017). Wnt/β-catenin signaling, disease, and emerging therapeutic modalities. *Cell*, *169*(6), 985-999.

Ohtomo, T., Nakao, C., Sumiya, M., Kaminuma, O., Abe, A., Mori, A., ... & Yamada, J. (2013). Identification of acyl-CoA thioesterase in mouse mesenteric lymph nodes. *Biological and Pharmaceutical Bulletin*, 36(5), 866-871.

Pedersen, L. B., Mogensen, J. B., & Christensen, S. T. (2016). Endocytic control of cellular signaling at the primary cilium. *Trends in biochemical sciences*, *41*(9), 784-797.

Pentinmikko, N., Iqbal, S., Mana, M., Andersson, S., Cognetta, A. B., Suciu, R. M., ... & Smolander, O. P. (2019). Notum produced by Paneth cells attenuates regeneration of aged intestinal epithelium. *Nature*, *571*(7765), 398-402.

Peregrina, K., Houston, M., Daroqui, C., Dhima, E., Sellers, R. S., & Augenlicht, L. H. (2015). Vitamin D is a determinant of mouse intestinal Lgr5 stem cell functions. *Carcinogenesis*, *36*(1), 25-31.

Progatzky, F., Shapiro, M., Chng, S. H., Garcia-Cassani, B., Classon, C. H., Sevgi, S., ... & Pachnis, V. (2021). Regulation of intestinal immunity and tissue repair by enteric glia. *Nature*, 1-6.

Rao, M., Nelms, B. D., Dong, L., Salinas-Rios, V., Rutlin, M., Gershon, M. D., & Corfas, G. (2015). Enteric glia express proteolipid protein 1 and are a transcriptionally unique population of glia in the mammalian nervous system. *Glia*, 63(11), 2040-2057.

Rescigno, M. (2008). News & Highlights: Don't forget to have a" second brain". *Mucosal Immunology*, 1(5), 328-329.

Rhee, S. H., Pothoulakis, C., & Mayer, E. A. (2009). Principles and clinical implications of the brain–gut–enteric microbiota axis. *Nature reviews Gastroenterology & hepatology*, 6(5), 306-314.

Ritter, A., Friemel, A., Kreis, N. N., Hoock, S. C., Roth, S., Kielland-Kaisen, U., ... & Yuan, J. (2018). Primary cilia are dysfunctional in obese adipose-derived mesenchymal stem cells. *Stem Cell Reports*, *10*(2), 583-599.

Romijn, J. A., Corssmit, E. P., Havekes, L. M., & Pijl, H. (2008). Gut–brain axis. *Current Opinion in Clinical Nutrition & Metabolic Care*, 11(4), 518-521.

Roulis, M., Kaklamanos, A., Schernthanner, M., Bielecki, P., Zhao, J., Kaffe, E., ... & Chalkidi, N. (2020). Paracrine orchestration of intestinal tumorigenesis by a mesenchymal niche. *Nature*, *580*(7804), 524-529.

Rühl, A. (2005). Glial cells in the gut. *Neurogastroenterology & Motility*, 17(6), 777-790.

Sato, T., Van Es, J. H., Snippert, H. J., Stange, D. E., Vries, R. G., Van Den Born, M., ... & Clevers, H. (2011). Paneth cells constitute the niche for Lgr5 stem cells in intestinal crypts. *Nature*, *469*(7330), 415-418.

Sawa, H. (2012). Control of cell polarity and asymmetric division in C. elegans. *Current topics in developmental biology*, *101*, 55-76.

Scadden, D. T. (2006). The stem-cell niche as an entity of action. *Nature*, *441*(7097), 1075-1079.

Shoshkes-Carmel, M., Wang, Y. J., Wangensteen, K. J., Tóth, B., Kondo, A., Massasa, E. E., ... & Kaestner, K. H. (2018). Subepithelial telocytes are an important source of Wnts that supports intestinal crypts. *Nature*, *557*(7704), 242-246.

Simons, B. D., & Clevers, H. (2011). Stem cell self-renewal in intestinal crypt. *Experimental cell research*, *317*(19), 2719-2724.

Singh, R. K., Chang, H. W., Yan, D. I., Lee, K. M., Ucmak, D., Wong, K., ... & Liao, W. (2017). Influence of diet on the gut microbiome and implications for human health. *Journal of translational medicine*, 15(1), 1-17.

Smillie, C. S., Biton, M., Ordovas-Montanes, J., Sullivan, K. M., Burgin, G., Graham, D. B., ... & Sud, M. (2019). Intra-and inter-cellular rewiring of the human colon during ulcerative colitis. *Cell*, *178*(3), 714-730.

Stark, K., Vainio, S., Vassileva, G., & McMahon, A. P. (1994). Epithelial transformation of metanephric mesenchyme in the developing kidney regulated by Wnt-4. *Nature*, 372(6507), 679-683.

Stzepourginski, I., Nigro, G., Jacob, J. M., Dulauroy, S., Sansonetti, P. J., Eberl, G., & Peduto, L. (2017). CD34+ mesenchymal cells are a major component of the intestinal stem cells niche at homeostasis and after injury. *Proceedings of the National Academy of Sciences*, *114*(4), E506-E513.

Ternet, C., & Kiel, C. (2021). Signaling pathways in intestinal homeostasis and colorectal cancer: KRAS at centre stage. *Cell Communication and Signaling*, *19*(1), 1-22.

Valenta, T., Degirmenci, B., Moor, A. E., Herr, P., Zimmerli, D., Moor, M. B., ... & Basler, K. (2016). Wnt ligands secreted by subepithelial mesenchymal cells are essential for the survival of intestinal stem cells and gut homeostasis. *Cell reports*, *15*(5), 911-918.

Van der Flier, L. G., Haegebarth, A., Stange, D. E., Van de Wetering, M., & Clevers, H. (2009). OLFM4 is a robust marker for stem cells in human intestine and marks a subset of colorectal cancer cells. *Gastroenterology*, *137*(1), 15-17.

Xavier, R. J., & Podolsky, D. K. (2007). Unravelling the pathogenesis of inflammatory bowel disease. *Nature*, *448*(7152), 427-434.

Yamada, J., Matsumoto, I., Furihata, T., Sakuma, M., & Suga, T. (1994). Purification and properties of long-chain acyl-CoA hydrolases from the liver cytosol of rats treated with peroxisome proliferator. *Archives of biochemistry and biophysics*, 308(1), 118-125.

Yamada, J. (2005). Long-chain acyl-CoA hydrolase in the brain. *Amino acids*, 28(3), 273-278.

Yang, J. L., Jiang, H., Pan, F., Ho, C. S., & Ho, R. C. (2016). The effects of high-fat-diet combined with chronic unpredictable mild stress on depression-like behavior and leptin/leprb in male rats. *Scientific reports*, *6*(1), 1-12.

Yilmaz, Ö. H., Katajisto, P., Lamming, D. W., Gültekin, Y., Bauer-Rowe, K. E., Sengupta, S., ... & Sabatini, D. M. (2012). mTORC1 in the Paneth cell niche couples intestinal stem-cell function to calorie intake. *Nature*, *486*(7404), 490-495.

Yoo, B. B., & Mazmanian, S. K. (2017). The enteric network: interactions between the immune and nervous systems of the gut. *Immunity*, 46(6), 910-926.

Zhang, Y., Li, Y., Niepel, M. W., Kawano, Y., Han, S., Liu, S., ... & Cohen, D. E. (2012). Targeted deletion of thioesterase superfamily member 1 promotes energy expenditure and protects against obesity and insulin resistance. *Proceedings of the National Academy of Sciences*, 109(14), 5417-5422.

Zhuravleva, E., Gut, H., Hynx, D., Marcellin, D., Bleck, C. K., Genoud, C., ... & Hemmings, B. A. (2012). Acyl coenzyme A thioesterase Them5/Acot15 is involved in cardiolipin remodeling and fatty liver development. *Molecular and cellular biology*, 32(14), 2685-2697.

Appendix I: IHC analysis of S100beta in colonic crypts.

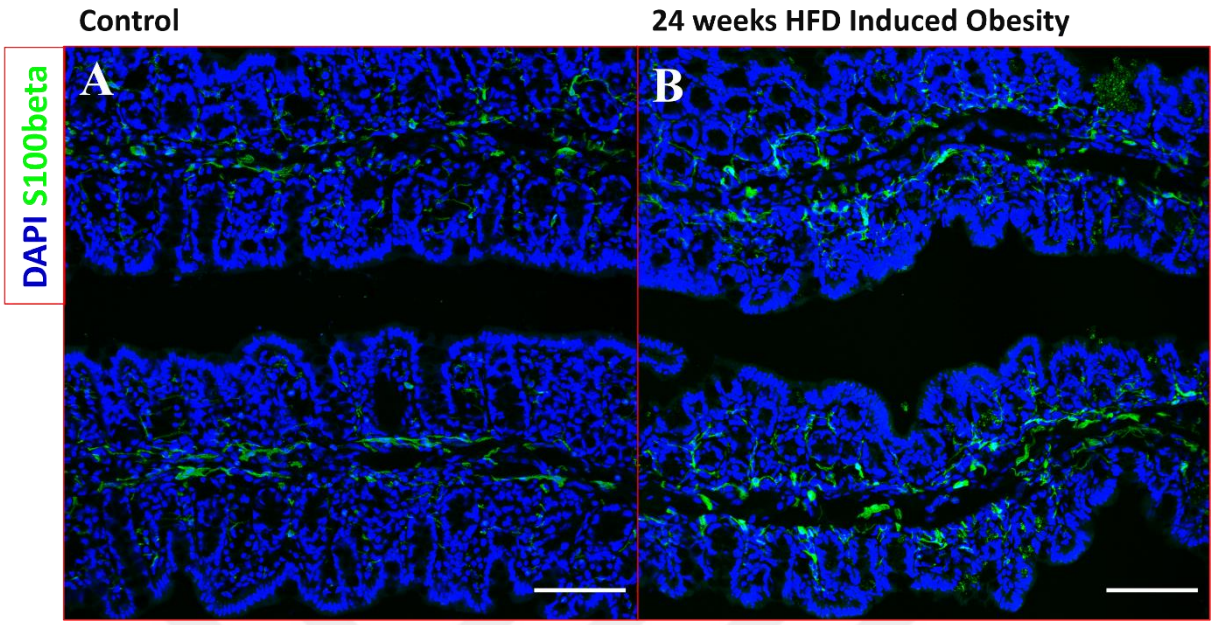

In high fat diet induced obesity model (B), glial cells around the crypts were detected by using S100beta (green) compared to control (A). Scale bar represents 150 µm.

Appendix II: IHC analysis of brain insular cortex region.

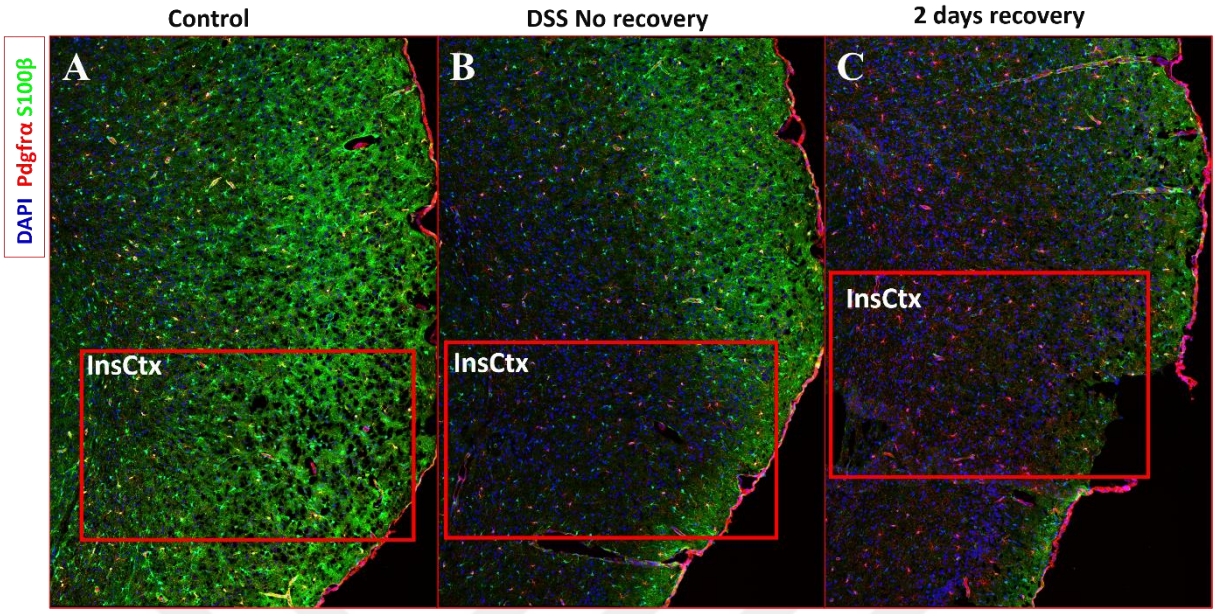

Tile Scan images of insular cortex regions of brain from control (A), DSS induced colitis (B) and recovery (C) animals show glial cells with S100beta (green) along with the PDGFRA expression (red).

Appendix III: IHC analysis of brain insular cortex region.

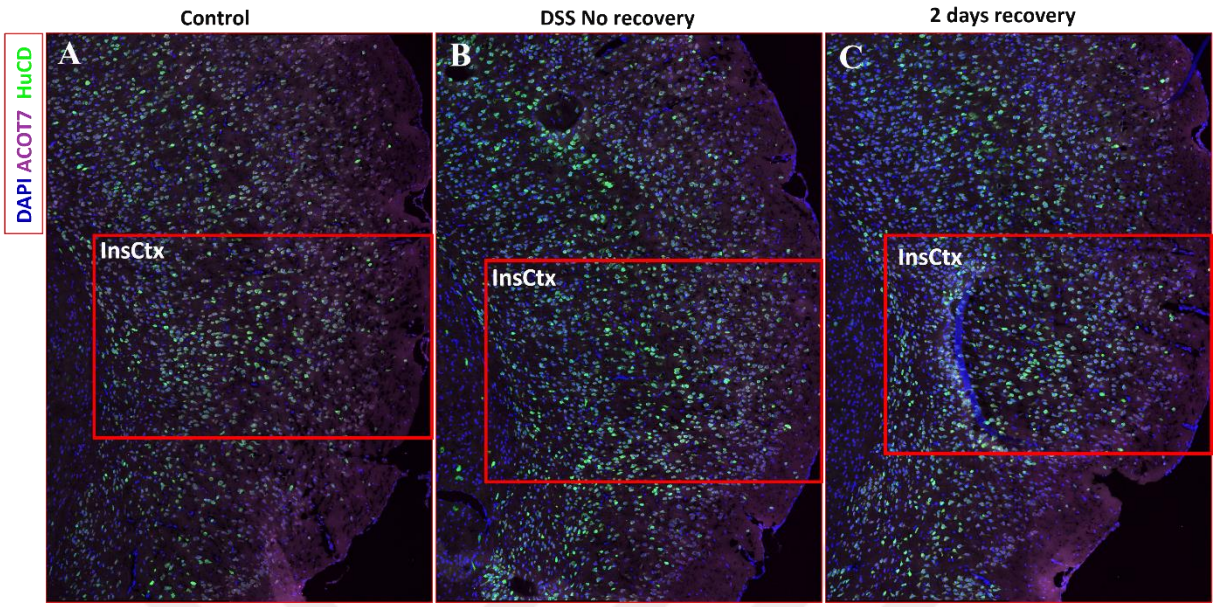

Tile Scan images of insular cortex regions of brain from control (A), DSS induced colitis (B) and recovery (C) animals show neurons with HuCD (green) along with the ACOT7 expression (magenta).

Appendix IV: List of primary and secondary antibodies used.

Antibody	Host	Clonality	Supplier	Catalogue Number	Dilution in Blocking Buffer
anti-Arl13b [N295B/66]	Mouse	Monoclonal	Abcam	ab136648	1:100
anti-Arl13b	Rabbit	Polyclonal	ProteinTech	17711-1-AP	1:1000
anti-ACOT7	Rabbit	Polyclonal	Sigma Aldrich	HPA025735	1:100
anti-Pdgfra	Goat	Polyclonal	R&D Systems	AF1062	1:50
anti-S100beta [EP1576Y]	Rabbit	Monoclonal	Abcam	ab52642	1:100
anti-HuCD [16A11]	Mouse	Monoclonal	Invitrogen	A21271	1:100
anti-Tuj1	Rabbit	Polyclonal	Biolegend	802001	1:100
anti-Sox10	Rabbit	Polyclonal	Invitrogen	PA5-40697	1:100
anti-Sox9	Rabbit	Polyclonal	Millipore	ab5535	1:100
anti-Muc2	Rabbit	Polyclonal	Abcam	ab97386	1:100
anti-Lysozyme [EPR2994(2)]	Rabbit	Monoclonal	Abcam	ab108508	1:100
anti-CD34 [EP373Y]	Rabbit	Monoclonal	Abcam	ab81289	1:100
anti-Beta catenin	Mouse	Monoclonal	BD Biosciences	610154	1:100
anti-E-cadherin	Mouse	Monoclonal	BD Biosciences	610182	1:50
anti-Ano2 (D-2)	Mouse	Monoclonal	Santa Cruz	SC390956	1:50
anti-PHOX2B	Goat	Polyclonal	R&D	AF4940	1:100
anti-PCNT	Rabbit	Polyclonal	Abcam	ab4448	1:100
anti-Vimentin	Rabbit	Polyclonal	Invitrogen	PA5-27231	1:100
anti-Actin,α Smooth Muscle (1A4)	Mouse	Monoclonal	Sigma Aldrich	A2547	1:100
anti-Choline Acetyltransferase	Goat	Polyclonal	Millipore	AB144P	1:100
anti-Olfm4 (D6Y5A)	Rabbit	Monoclonal	Cell Signalling	39141	1:100
anti-Ki67 [SP6]	Rabbit	Monoclonal	Abcam	ab16667	1:100
Cy2 Conjugated AffiniPure Donkey anti-Mouse IgG (H+L)	Donkey	Polyclonal	Jackson Immuno Research	715-225-151	1:400
Cy3 Conjugated AffiniPure Donkey anti-Mouse IgG (H+L)	Donkey	Polyclonal	Jackson Immuno Research	715-165-151	1:400
Cy3 Conjugated AffiniPure Donkey anti-Rabbit IgG (H+L)	Donkey	Polyclonal	Jackson Immuno Research	711-165-152	1:400
Cy5 Conjugated AffiniPure Donkey anti-Rabbit IgG (H+L)	Donkey	Polyclonal	Jackson Immuno Research	711-175-152	1:400
Cy5 Conjugated AffiniPure Donkey anti-Goat IgG (H+L)	Donkey	Polyclonal	Jackson Immuno Research	705-175-147	1:400

This list provides information on the antibodies used in this thesis with great detail in immunohistochemical (IHC) analysis.

Appendix V: IHC analysis of small intestine and colon in 24 weeks Western Diet.

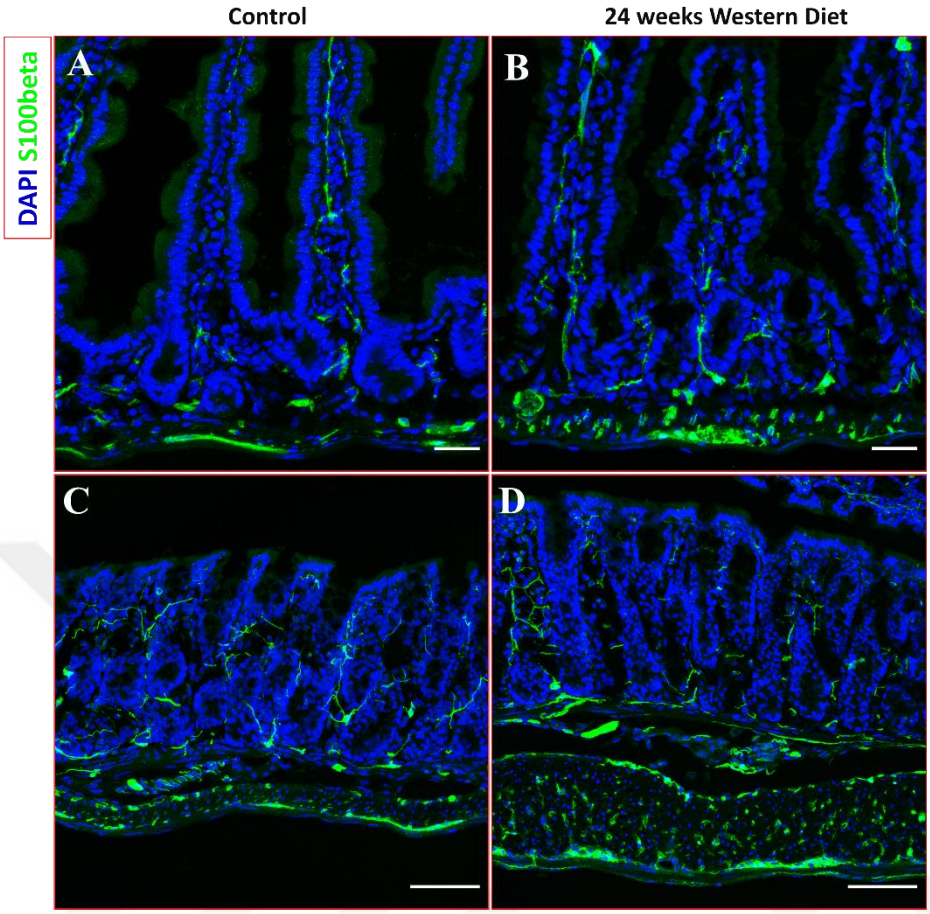

Western Diet model with prolonged western diet administration in small intestine(A,B) and colon (C,D). Glial cells around the crypts were detected by using S100beta (green). Scale bar represents 50 µm (A,B), 150 µm (C,D).

Appendix VI: IHC analysis of small intestine and colon in 24 weeks Western Diet.

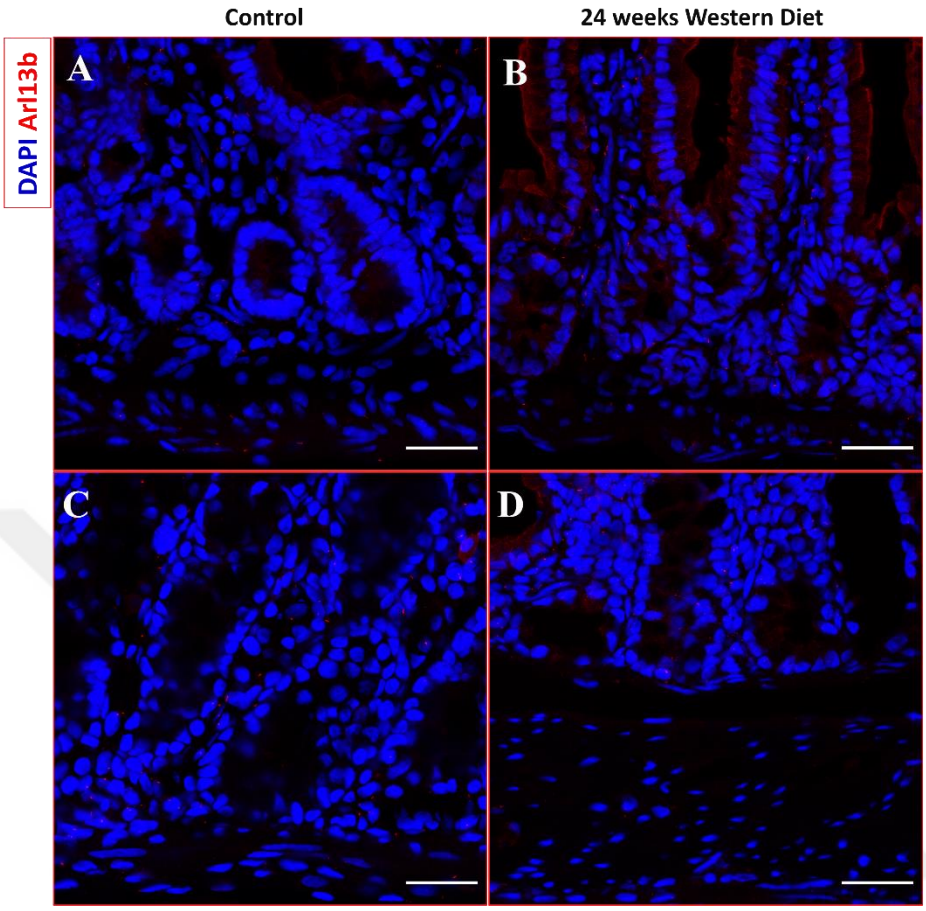

Western Diet model with prolonged western diet administration in small intestine(A,B) and colon (C,D). Primary cilia structures around the crypts and in myenteric plexus were detected by using Arl13b (red). Scale bar represents 50 µm.